Univerza
v Ljubljani
Fakulteta
*za gradbeništvo
in geodezijo*

*ODDELEK ZA
GEODEZIJO*

*UNIVERZITETNI
ŠTUDIJ GEODEZIJE
SMER GEODEZIJA*

Kandidatka:

ANA URBAS

VPLIV INSTRUMENTALNIH POGREŠKOV NA SATELITSKI ZAJEM PORAZDELITVE ANTROPOGENIH PLINOV V ATMOSFERI

Diplomska naloga št.: 874

EFFECTS OF INSTRUMENTAL ERRORS IN THE RETRIEVAL OF ANTHROPOGENIC GAS DISTRIBUTION FROM SATELLITE

Graduation thesis No.: 874

Mentor:
Izr.prof.dr. Krištof Oštir

Predsednik komisije:
Izr.prof.dr. Dušan Kogoj

Somentor:
Dr. Luca Maresi

Ljubljana, 2. 12. 2011

ERRATA

Page	Line	Reads	Should Read

STATEMENTS

I, the undersigned Ana Urbas, declare that I am the author of graduation thesis entitled »Effects of instrumental errors in the retrieval of anthropogenic gas distribution from satellite«.

I declare that the electronic version is exactly the same as printed version.

I declare that I allow the publication of the electronic version of my graduation thesis in the repository of UL FGG.

Ljubljana, 15.11.2011   Ana Urbas

BIBLIOGRAPHIC-DOCUMENTALISTIC INFORMATION AND ABSTRACT

Abstract

In this thesis the remote sensing is presented as a method for observing the distribution of trace gases in the Earth's atmosphere. In theoretical basis, the focus is set to the absorption spectroscopy, which makes use of absorption fingerprints of molecules to detect different gases. Four current hyperspectral satellite instruments are described that work on the principle of spectroscopy – GOME, SCIAMACHY, OMI and TROPOMI. In the practical part of the thesis analyses of the effect of the instrumental errors on trace gas retrieval are described as well as their results. Analyses have been done in the framework of TROPOMI development project with TIDE software. TIDE simulates the retrieval of trace gases with TROPOMI and was developed especially for this project.

BIBLIOGRAFSKO-DOKUMENTACIJSKA STRAN IN IZVLEČEK

Izvleček

V diplomski nalogi je obravnavano daljinsko zaznavanje kot metoda za opazovanje porazdelitve in gostote antropogenih plinov v Zemljini atmosferi. Podrobneje so predstavljene teoretične osnove spektroskopije, ki sestavne elemente ozračja zaznava na podlagi njihovih absorpcijskih spektralnih podpisov. Opisani so štirje aktualni hiperspektralni satelitski instrumenti za opazovanje ozračja, ki delujejo po principu spektroskopije – GOME, SCIAMACHY, OMI in TROPOMI. V praktičnem delu naloge so predstavljene analize vplivov instrumentalnih pogreškov, kot so šum, razpršena svetloba ter netočna registracija valovnih dolžin, ter njihovi rezultati. Analize so bile narejene v okviru projekta razvoja novega instrumenta TROPOMI s posebej za ta namen razvitim programom TIDE, ki simulira delovanje instrumenta.

ACKNOWLEDGMENT

TABLE OF CONTENTS

TABLE OF TABLES

TABLE OF FIGURES

ABBREVIATIONS AND SIMBOLS

AMF	Air Mass Factor
BOL	Beginning of Life
CCD	Charged Coupled Device
DIAL	Differential Absorption Lidar
DOAS	Differential Optical Absorption Spectroscopy
EM	Electromagnetic
ENVISAT	Environmental Satellite
EOL	End of Life
EOS	Earth Observation System
ERS	European Remote Sensing Satellite
ESA	European Space Agency
ESTEC	European Space Research and Technology Centre
FOV	Field of View
GOME	Global Ozone Monitoring Experiment
GUI	Graphical User Interface
IFOV	Instantaneous Field of View
IR	Infrared
KNMI	The Royal Dutch Meteorological Institute
LASER	Light Amplification by Stimulated Emission of Radiation
LEO	Low Earth Orbit
LIDAR	Light Detection and Ranging
METOP	Meteorological Operational Satellite
NASA	National Aeronautics and Space Administration
NIR	Near Infrared
OMI	Ozone Monitoring Instrument
QE	Quantum Efficiency
RMS	Root Mean Square
RTM	Radiative Transfer Model
S-5P	Sentinel-5 Precursor
SCD	Slant Column Density
SCIAMACHY	Scanning Imaging Absorption Spectrometer for Atmospheric Cartography
SI	International System of Units
SNR	Signal to Noise Ratio
SRON	Netherlands Institute for Space Research
SWIR	Short Wave Infrared

RADAR	Radio Detection and Ranging
TIDE	TROPOMI Integrated Development Environment
TIROS	Television and Infrared Observation Satellite
TROPOMI	Tropospheric Ozone Monitoring Instrument
UV	Ultraviolet
VCD	Vertical Column Density
VIS	Visible light
2D	Two-dimensional

1   **INTRODUCTION**

The Earth's atmosphere functions as a combined life support system and protective shield. It supplies us with the air we breathe and protects us against harmful radiation. However, the composition of this important layer is changing and the long term consequences are unknown.

Nowadays we can witness more and more weather extremes – blizzards, floods, droughts, heat waves and heavy winds. Those events that are every year more punishing are believed to be the consequence of global warming. Global warming is to a great extent caused by human activity and his way of life by the emission of greenhouse and toxic gases in the atmosphere. Human activities have always interacted with the atmosphere but the growth of population and industrialisation in the 19th and 20th century has led to dramatic changes in the Earth system. Many species and ecosystems on the Earth are already being endangered by anthropogenic climate changes. Other consequences are acid rain, the depletion of the ozone layer and global increase of asthma rates. Therefore, different conventions, protocols and amendments about the reduction of greenhouse gases release were adopted in the nineties by United Nations. The most important among them are the Vienna Convention for the protection of the ozone layer (1992), Montreal protocol on substances that deplete the ozone layer (1992) and United Nations framework convention on climate change (1995) with Kyoto Protocol on greenhouse gas emission reduction (2002) (MOP, 2011).

To answer the questions of the problem of global climate change adequately and to ensure accurate remedies are taken, fairly good understanding of the gases present in the atmosphere is needed – changes in their concentration over time and chemical reactions that occur among those gases. Until recently, most of those questions could not have been answered. Today, however, manned aircraft, rockets, and satellites are able to collect important data for the scientists to model the future behaviour of the atmosphere, to understand the historic development of climate, to monitor anthropogenic and natural emissions as well as to collect knowledge for policy makers to facilitate their decisions. The most important is space-borne monitoring from satellites. It provides global coverage with high (daily) temporal resolution. In addition, compared to other platforms satellites provide more data in the same temporal interval and cover also remote and inaccessible area such as oceans, deserts, mountains and poles. Global monitoring of the atmosphere makes it possible to find and to locate sources of different emissions, and to supervise the implementation of conventions rules. Better understanding of chemical reactions in the atmosphere has a significant impact on assessment of the impact that they have on the weather and climate.

Space-borne observations of the atmosphere have been continuously ongoing since 1960 when the first meteorological satellite TIROS 1 (Television and Infrared Observation Satellite) was launched by NASA. Its prior mission was to photograph the clouds pattern. Since then a series of satellites for

detection of different atmospheric characteristics has been launched by national agencies from all over the world. One of the leading agencies in this field is also the European Space Agency (ESA). Today ESA, in cooperation with Dutch national institutes, is developing a new space-borne instrument TROPOMI for the atmospheric observations due to launch in 2014.

I got the opportunity to spend five months, from November 2010 to April 2011, as a trainee at ESA's European Space Research and Technology Centre (ESTEC) in Holland. During this period I was working on the TROPOMI project, a development of a hyper spectral spectrograph that will use an absorption spectroscopy to detect vertical profiles of different trace gases in the atmosphere. I was impressed by the new application of remote sensing which I have not met before during my studies but is, at the same time, helping to understand one of the topical issues in modern society better – the problem of global warming and climate changes. During my stay at ESTEC the TROPOMI developing group of scientists welcomed me and let me cooperate in this mission. On their meetings I have learned about the project work, I gained an overview of the phases of such a project and an insight in the amount and diversity of work, which is hidden behind every satellite mission. I decided to present my contribution in this project in my diploma thesis. On this topic I also wrote an article which I presented at the EARSeL 7th SIG-Imaging Spectroscopy Workshop in Edinburgh in April 2011 and was published in the conference proceedings (Urbas, Esposito, de Vries, 2011).

The geodetic community considers remote sensing as a technique for the observation of the Earth's surfaces. But it is equally powerful when used to detect the characteristics of the media the electromagnetic radiation is traversing – to detect the composition of the atmosphere and the horizontal and vertical distribution of its constituents – gases, aerosols and clouds. In this work I would like to present the theoretical background of remote sensing of the atmosphere using differential optical absorption spectroscopy (DOAS) to detect even the gases with very low mixing ratio which are present only in traces – the so called trace gases. In the practical part of my thesis the work I did during my stage at ESTEC is presented. I was using a software tool TIDE that simulates the expected performance of TROPOMI to assess how the instrument noise and the stray light will affect the retrieved vertical columns of different gases. In the research the impacts of spectral mis-registration and of the aging of the instrument have also been assessed. During my work with TIDE a bug was found in the system, therefore I contributed my share also to the upgrade of TIDE.

The outline of this work is as follows: the *first chapter* is the introduction presenting the motivation and the goals of my research and thesis, the structure of the work is shortly described. In the *chapter two* the remote sensing of the atmosphere is presented, starting with its history and its technological development. Different platforms, methods and sensors used for atmospheric observation are presented as well as the structure and the composition of the Earth's atmosphere.

Chapter three deals with the fundamentals of atmospheric radiation and physics, with the aim of introducing some important aspects necessary to understand the research presented in this thesis. The main aspects are basic radiation laws, processes that attenuate the solar radiation, such as scattering and absorption by gases and particles, and the formation of absorption lines, the identifiers of atmospheric constituents.

Chapter four illustrates briefly the optical instruments for detection of gas concentration. Described are the concepts of spectroscopy and spectrometer, more attention is paid to the technique DOAS. Furthermore, in *chapter five*, the most technically improved space-borne instruments for atmosphere sounding that are still in use and are using absorption spectroscopy for gas detection (GOME, OMI, SCIAMACHY and TROPOMI) are presented.

In *chapter six* the TIDE software used for the analyses that were done to estimate the impact of some instrumental errors on the retrieval of gas profiles with TROPOMI is presented. The analyses and their results are described in *chapter seven*. The impact of noise, stray light and mis-registration are discussed. *Chapter eight* concludes the thesis. *Chapter nine* is the summary of the whole thesis in Slovene language.
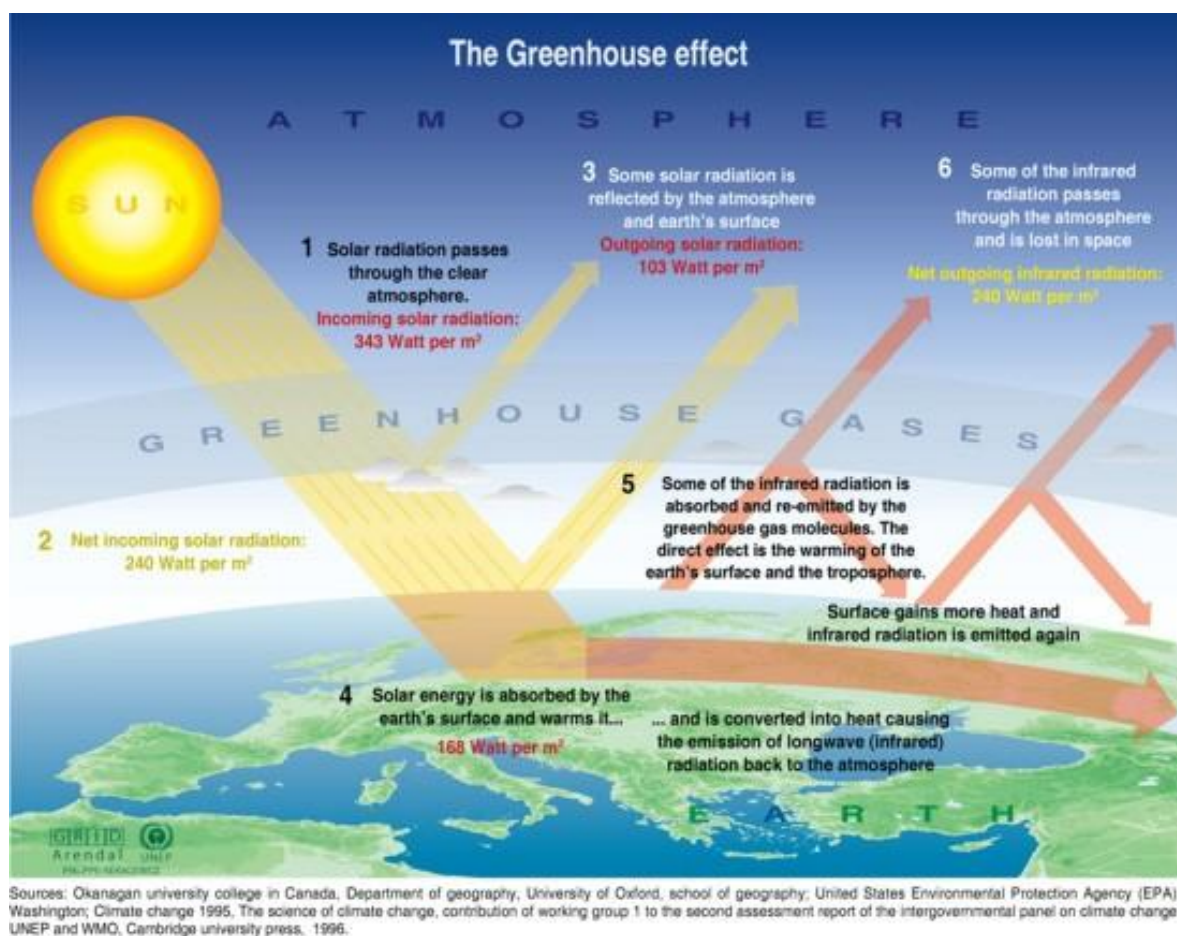
Figure 1: The greenhouse effect (http://wwwp.dailyclimate.org/tdc-newsroom/2011/08/carbon-facts-dont-tell-the-whole-story, 26.9.2011).

2   REMOTE SENSING OF THE ATMOSPHERE

Sensing the composition of the atmosphere is mapping the invisible to the human eye, enabled with today's technology. Space-borne atmospheric sensors can map the atmosphere in three dimensions, producing high-resolution horizontal and vertical cross-sections of trace chemicals, dust particles and clouds, from ground level to a hundred kilometres in the air.

This chapter firstly presents the chemical composition of the Earth's atmosphere – its basic constituents and the layers the atmosphere is divided in due to different physical characteristics. Furthermore, the history of atmospheric remote sensing is described. The main topic of this chapter, however, is the presentation of different techniques and sensors that are in use for remote sensing of the atmosphere.

2.1   Composition of Earth's atmosphere

The atmosphere is a layer of gases surrounding the Earth retained by Earth's gravity. The atmosphere enables life on Earth by absorbing dangerous ultraviolet solar radiation, warming the surface through heat retention and reducing temperature extremes between day and night. Without atmosphere the temperature on the Earth's surface would be balanced with the Sun's radiation, i.e. approximately 240°K or –18°C. The gases in the atmosphere, especially water vapour, carbon dioxide and methane, absorb the Sun's radiation and keep the average temperature on the Earth around pleasant 15°C (SKP, 2010). This natural phenomenon of conserving the heat in the atmosphere is called greenhouse effect. The present atmosphere is thought to be developed mainly from gases ejected by volcanoes.

Earth's atmosphere is composed of about 78% nitrogen, 21% oxygen, and 0.93% argon. The remainder, less than 0.1%, contains many small but important trace gases, including water vapour, carbon dioxide, methane and ozone. The chemical composition of the atmosphere does not vary with altitude. All of these trace gases have an important effect on the Earth's climate.

Table 1: The composition of the atmosphere. Units ppmv and ppbv stand for parts per million by volume and parts per billion by volume. (Javed 2009)

Constituents	Tropospheric mixing ratio
N_2 (Nitrogen)	78.08%
O_2 (Oxygen)	20.95%
H_2O (water vapor)	<3.00%
A (Argon)	0.93%
CO_2 (carbon dioxide)	345 ppmv
O_3 (ozone)	10 ppmv
CH_4 (methane)	1.6 ppmv
N_2O (nitric oxide)	350 ppbv
CO (carbon monoxide)	70 ppbv
CFC's	0.2-0.3 ppbv

The atmosphere can be divided into layers determined by the way temperature changes with height. The layer closest to the surface is the troposphere, which contains over 80% of the atmospheric mass and nearly all water vapour and air pollution (pollution gases and aerosols). It is about 11 km thick, thinner at poles (about 8 km) and thicker at equator (about 16 km). In troposphere all clouds and weather occur. Within this layer the temperature drops with increasing height at an average rate of about 6.5°C per every 1000 m. The upper limit of the troposphere is called tropopause.

The next layer, the stratosphere, contains most of the atmosphere's ozone, which absorbs dangerous ultraviolet radiation from the Sun and makes life on the Earth possible. The stratosphere is found from about 11 to 48 km above the Earth's surface. The temperature slightly increases with altitude. The highest temperature in this region is about 0°C. Stratosphere ends with the stratopause.

Above the stratosphere is the mesosphere. Here, the temperature again decreases with altitude. In mesosphere, between 50 and 85 km above the Earth, most comets that fall on the Earth burn completely.

Above the mesopause, which concludes the mesosphere is the thermosphere, the highest layer of the Earth's atmosphere. It extends approximately to the height of 110 km. It is difficult to draw the line where the space starts but the fact is that at about this height the landing space shuttles start feeling the first atmospheric impacts. The temperature again starts increasing with altitude. Beyond the thermosphere is exosphere which is no longer considered as a part of the Earth's atmosphere.

Mesosphere and thermosphere include regions of charged atoms and molecules, or ions, therefore are often called the ionosphere. The air here is ionized by the Sun's UV light. These ionized layers affect the transmittance and reflectance of the radio waves.
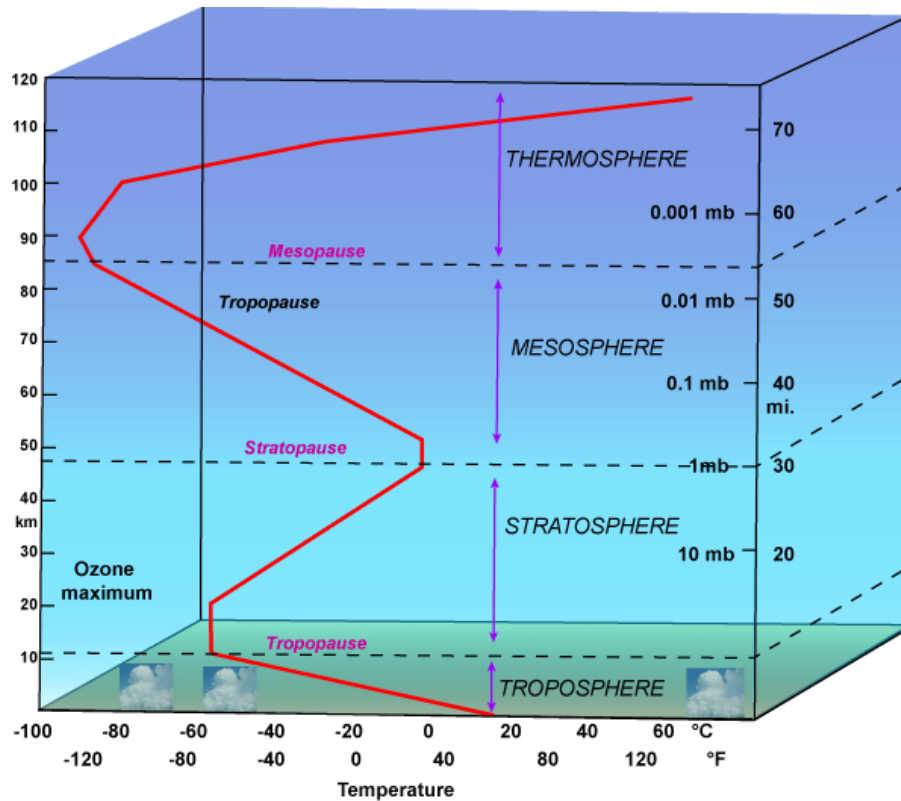
Figure 2: Layers of Earth's atmosphere and the way how the temperature changes with height (Lyndon State College, 2010).

2.2   Beginnings of the observation of the atmosphere

The fundamental principles for atmospheric observations were discovered during seventeenth and eighteenth century – in 1643 the Italian physicist Evangelista Torricelli invented the first barometer, while the air hygrometer, a device for measuring atmospheric humidity, was first constructed by Swiss physicist Horace Bénédict de Saussure in about 1780. At that time these instruments could only be used on the ground.

An important breakthrough in atmospheric observation came in the late eighteenth century with the invention of the hot-air balloon. In 1785 the English physician John Jeffries carried a thermometer, barometer, and hygrometer to a height of 2700 m in his balloon. For the next 150 years, balloons were the primary means used to carry instruments to the upper layers of the atmosphere.

With the payload development also measurement instruments developed and were able to measure more and more atmospheric characteristics, including its chemistry. One of the earliest examples of such research dates to 1804 when the French physicist Joseph Louis Gay-Lussac travelled in a balloon to a height of 6900 m to collect an air sample from this altitude. Upon his return to the ground Gay-Lussac analyzed this sample and concluded that the composition of air at 6900 m was the same as it was at sea level (Atmosphere Observation, 2010).

Later the airplanes and rockets replaced balloons, as they were able to reach much higher altitudes. But balloons did not go into oblivion. So-called sounding balloons are still regularly used to study the properties of the upper atmosphere.

The era of space-borne atmospheric observation started with the first weather satellite TIROS 1 (Television and Infrared Observation Satellite), launched by the U.S. government in 1960. One of its primary functions was to collect and transmit photographs of the Earth's cloud patterns. From that time till now several meteorological satellites were launched not only by NASA, but also by Russia, ESA, Japan, India and China (Atmosphere Observation, 2010).

2.3   Remote sensing platforms

Remote sensing/sounding can be performed from many platforms:

- ground,
- balloons,
- aircraft,
- rockets,
- space shuttle, and
- satellites.

In this thesis the focus is on space-borne remote sounding, i.e. from satellites.

At *ground-based measurements* the instrument is located on the ground and that is where the atmosphere is being sounded from. Ground-based measurements can provide long time series and high temporal resolution. This approach enables simultaneous measurements of many trace gases under well-calibrated conditions. It is used for comparison and development of different techniques and for the validation of new space-borne instruments. The main disadvantage of this method is the limited area it can cover.

**Figure 3: Telescope of a ground-based spectrometer for the remote sensing of greenhouse gases.
(KIT, 2011)**

Balloons can carry a variety of instruments, reaching the total weight up to several tones. Reaching altitudes of 40 km they provide height-resolved measurements. These large payloads are usually recovered after use. Compared to rockets and satellites balloons are inexpensive but more expensive than ground-based measurements. Balloons also do not provide global view or long time series. The dependence on meteorological conditions is strong.

**Figure 4: Launch of a super-pressure high-altitude stratospheric balloon for providing
meteorological and chemical information over Antarctica, 2010**

Measurements from *aircraft* are mainly used to validate satellite observations over a broad range of latitudes and altitudes. Aircraft measurements are obtained in campaigns with specially equipped high altitude aircraft.

Space-borne measurements provide comprehensive coverage and sampling. Global coverage makes it possible to monitor global distribution of atmospheric constituents, their evolution and propagation. All parts of the Earth can be observed regularly, also areas that are otherwise more or less inaccessible (poles, oceans, deserts). Observations from satellites can provide total column or height-resolved measurements. The main drawbacks of space-based performance are high price and higher risk. The repairs and upgrading of spacecraft are not possible after launch. In addition, complex space-qualified instrumentation and materials are required. Satellite's lifetime is usually limited to a few years.

Space-borne observations are being routinely used in wide variety of applications: atmospheric science, meteorology and climatology, agriculture, forestry, botany, planning applications, geodesy, geology, hydrology, oceanography, glaciology, mapping, disaster control, military applications, archaeology, etc.

To be sure that the data obtained by satellites orbiting few hundreds of kilometres above the Earth is credible, the continuous validation is needed. The satellite measurements are compared with other satellite-, aircraft-, balloon-, and ground-based measurements. Validation continues throughout the life of a satellite mission because instruments characteristics can change while in orbit.

Figure 5: Space-borne remote sensing
(http://www.atmos.illinois.edu/research/06remotesens.html, 21.6.2011)

2.4   Remote sensing techniques for trace gases detection

Remote sensing techniques are very common in places where direct access is not possible. This generally involves the measurement of electromagnetic (EM) radiation that has interacted with the object or medium of interest. EM radiation is used as an information-carrier. On the basis of the source

of this EM radiation, of the type of measurements, and of the spectral region remote sensing/sounding techniques can be classified as:

- active vs. passive,
- imaging vs. non-imaging vs. sounding, and
- according to the wavelength of radiation measured.

An imaging system measures the intensity of radiation, reaching it as a function of position on the Earth's surface so that a 2D picture of the intensity can be constructed. It can employ active or passive RS. A non-imaging system either does not measure the intensity of radiation or does not do so as a function of position on the Earth's surface. A sounding system ("sounder") measures the intensity of radiation to provide information about a particular property as a function of height in the atmosphere.

Using these three ways of classifying remote sensing, Kimberly Strong, professor of physics on University of Toronto, constructed a ″family tree″ of techniques, which is presented on the

Figure 6 and shortly described in the following pages. With red the technique used by space-borne instruments for trace gas detection, presented in the chapter 5, is indicated.
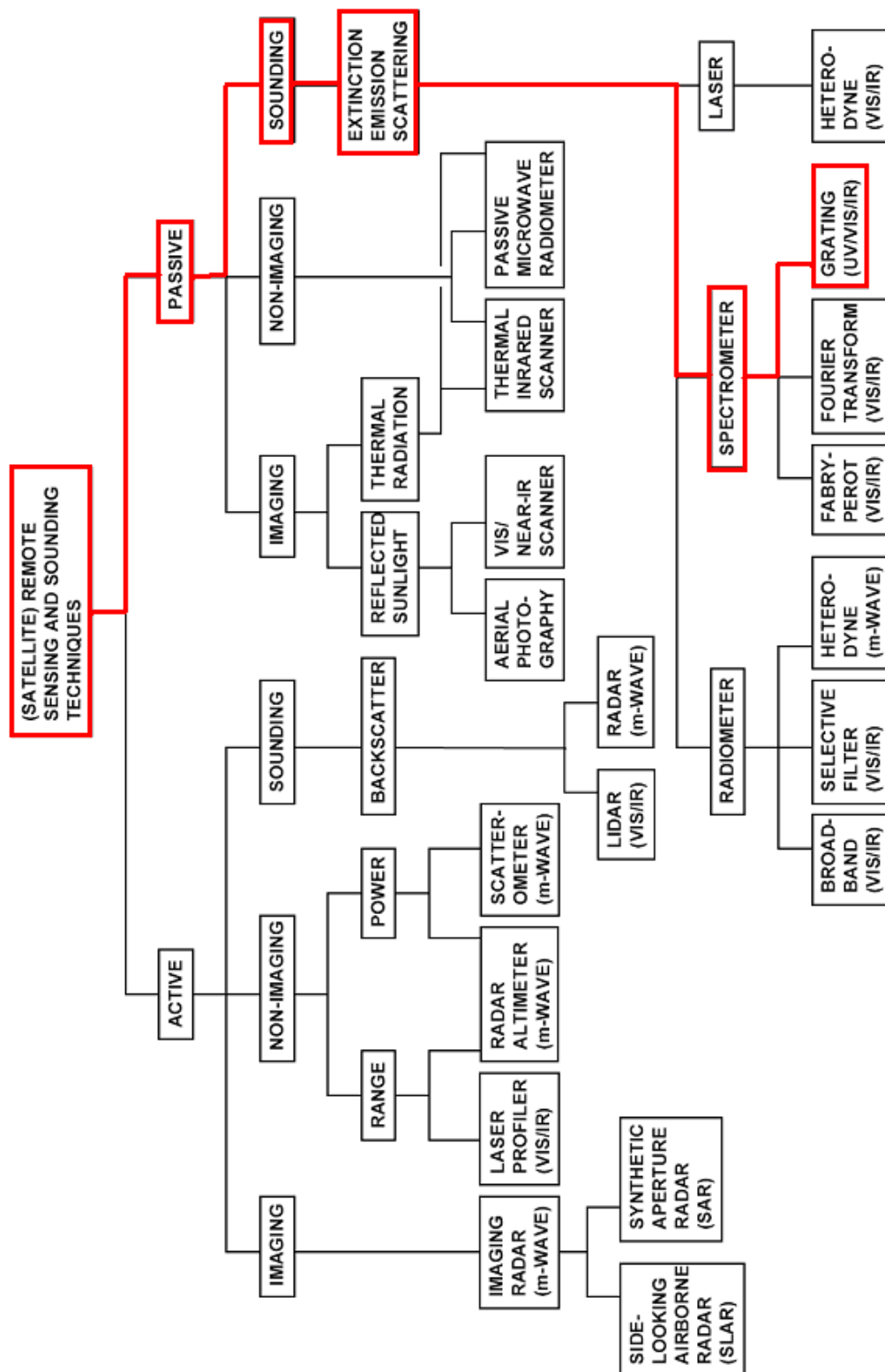
Figure 6: Family tree of remote sensing techniques. With red line the technique used by space-borne spectrometers for trace gas detection, presented in this thesis, is indicated.

Figure 6 shows a list of techniques, though not all of them can be used in atmospheric observations. Imaging techniques, neither active nor passive, do not provide any information on atmospheric parameters, except in the case of the image of cloud pattteren. Non-imaging active techniques are also not appropriate for this purpose. Passive non-imaging techniques, on the other hand, can be used to measure different properties of the atmosphere as well as passive and active sounding techniques. Below is a brief description of useful techniques.

2.4.1   Passive non-imaging system

Passive non-imaging system includes the thermal IR scanner and the passive microwave radiometer, which is not used in imaging mode. Thermal IR scanners can be used in non-imaging mode to measure temperature, pressure, humidity, and composition of the atmosphere (which overlaps with sounding), while passive microwave radiometers can be used in this mode to measure wind speed over oceans, atmospheric water vapour, cloud liquid water content, rainfall rate, and temperature.

In the atmospheric research, sounding techniques, active and passive, are even more useful than the above mentioned non-imaging observations.

2.4.2   Passive sounding system

Sounding is a measurement of vertical distribution of physical properties. Passive sounding systems generally measure the extinction, emission, or scattering of radiation in order to retrieve atmospheric properties. On the basis of spectral resolution they can be classified in three groups:

- radiometers,
- spectrometers, and
- monochromatic laser techniques.

Spectrometers are believed to be the most promising technique for remote detection of trace gases in the Earth's atmosphere. They disperse natural radiation into its constituent wavelength over a finite spectral range. Instrument measure the radiance reflected from the Earth that has undergone the absorption by different gases in the atmosphere. Each detected wavelength is compared to the reference radiation of the same wavelength (Sun irradiance without traversing the atmosphere or internal light source). Each trace gas absorbs only certain wavelengths of EM radiation and those fingerprints are known. According to the result of the comparison of both radiations the presence and the concentration of individual trace gases is derived. The biggest advantage of spectrometers to other techniques is that they allow detection of numerous species at the same time.

There are three types of spectrometers in use:

- *Prism spectrometer* – that simply use a prism to disperse the light, each wavelength being refracted at a different angle determined by the index of refraction of the prism (used in ground-based instruments, not on satellites).
- *Grating spectrometers* – that use a diffraction grating instead of the prism to disperse the wavelengths. Diffraction grating is an optical element, which consists of equally spaced parallel grooves, formed on a reflective coating. The polychromatic light incident on the grating is dispersed so that each wavelength is reflected from the grating at a slightly different angle. It is widely used in remote sounding satellites instruments to measure atmospheric temperature, composition, and aerosol properties, and to study ocean colour (differentiates between organic and inorganic materials in the water).
- *Interferometers* – that use interference effects to obtain spectral information.

For a more detailed description of spectrometers see chapter 4.2.
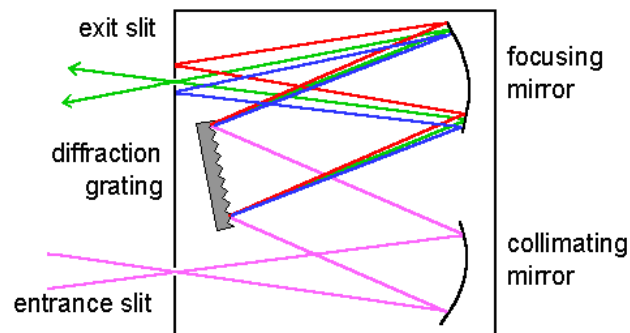
Figure 7: Diffraction grating spectrometer (Virginia Tech, 2011).

2.4.3   Active sounding systems

Active remote sensing techniques use artificial radiation; this can be either radio (microwave) spectrum – radar (Radio Detection and Ranging), or visible and infrared spectrum – laser (Light Amplification by Stimulated Emission of Radiation) or lidar (Light Detection and Ranging).

Active sounding system use radar and visible/infrared lasers (lidar). Pulses or continuous signals are transmitted, backscattered, and received. However, the target is the atmosphere, not the Earth's surface. Information is obtained from:

- the strength of the backscattering (related to density, size, distribution, and shape of the scattering particles);

- the absorption of the beam on its path to and from the target (related to the concentration and distribution of the absorbers);

- the polarization of the backscattered radiation (related to the properties of the target and of the absorbers);

- the change in phase after backscattering;

- the spectral broadening of pulses after backscattering from particles of different masses.

There are two active sounding techniques:

a)   Radar

Weather radar is used to detect precipitation. It can be used in ground-based networks or on satellites. Doppler radar is used to measure wind speed and direction from the Doppler shift in frequency between the transmitted and received signals. It has not yet flown on satellite.

b)   Lidar

Lidar is used to measure aerosol backscatter, concentrations of H_2O and O_3, temperature profiles, winds and cloud properties. It has also not flown on the satellite yet.

There are two basic lidar techniques, differential absorption lidar (DIAL) and Raman lidar. The DIAL technique employs two laser wavelengths to estimate atmospheric trace gas number density. One wavelength is selected to coincide with the centre of a molecular absorption line while the second wavelength is selected to fall in a nearby non-absorbing region. If they are within a few cm^{-1} of one another, then the elastic scattering (Raylight and Mie scattering; see section 3.4) properties of the atmosphere are assumed to be identical and can be neglected. Laser power at both wavelengths is transmitted into the atmosphere (either simultaneously or sequentially) and is elastically scattered into the field of view (FOV) of the lidar receiver. The DIAL technique can be used to estimate the number density of absorber molecules at a specific range or the average over a path (GRSS, 2009).

The Raman lidar technique involves detecting transmitted laser radiation, which has been shifted in wavelength due to interaction with the scattering molecule (Raman scattering; see section 3.4). The backscattered power of the wavelength shifted signal is proportional to the concentration of scattering molecules. Raman lidar offers a direct measure of species concentration or mixing ratio by comparing the Raman signal of the scatterer to the Raman signal of N_2 or O_2 (GRSS, 2009).
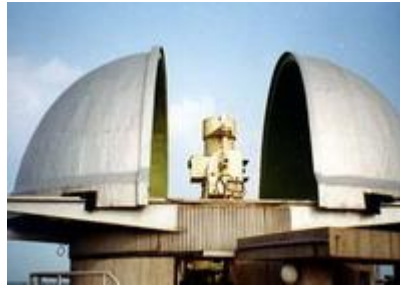
Figure 8: The lidar system for the atmospheric sounding (Hefei, 2010).
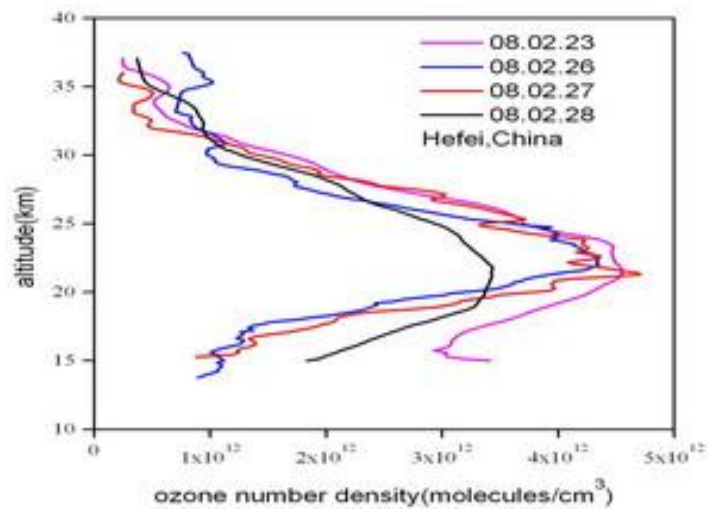
Figure 9: Lidar measurement of stratospheric O_3 (Hefei, 2010).

Trace gases are the most variable constituents of the atmosphere both temporally and spatially. Certain trace gases, primarily water vapour, CO_2, CH_4 and to a lesser extent O_3 and N_2O, have strong absorption features in the near to mid infrared. Variations in the atmospheric concentration of these trace gases may lead to significant global climatological change by altering the absorption and re-radiation of long wave terrestrial radiation (greenhouse effect). The constituent gases (oxygen and nitrogen) are well mixed and therefore their abundance can be calculated accurately from the measurement of atmospheric pressure alone. Trace gas concentration, however, must be measured directly using either in-situ methods or remote sensing methods to record their distribution and fluctuations. Long term global monitoring of trace gases is needed to further improve modelling of global change processes. Global coverage obtained by satellite observations also provides the information on spatial patterns of different gases so that a specific origin can be directly assigned to an

observed phenomenon (e.g. enhanced trace gas concentrations above an industrialized area, emission of NO_2 caused by ship traffic on the oceans).
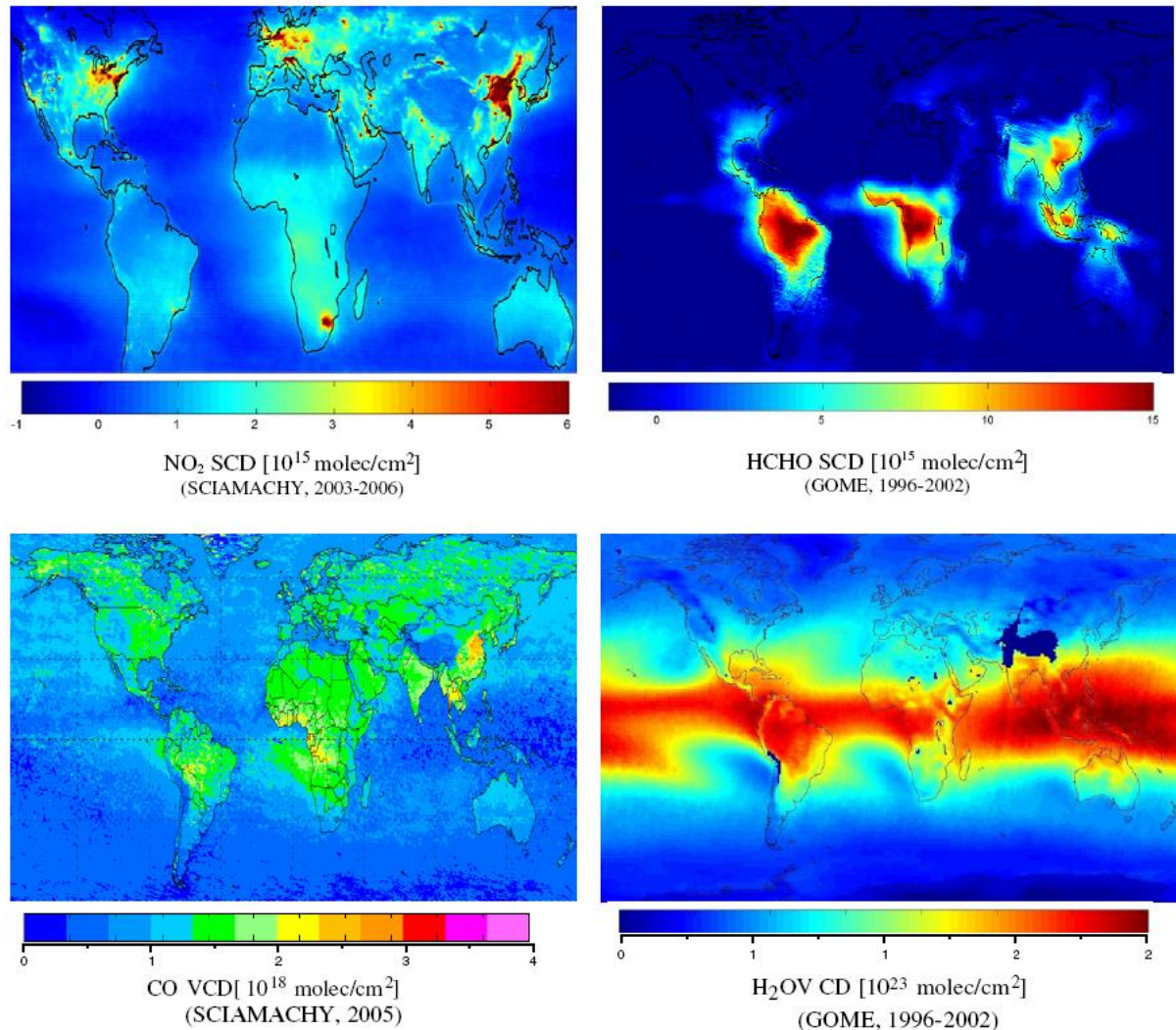
Figure 10: Global distribution of tropospheric NO_2, formaldehyde (HCHO), carbon monoxide (CO) and water vapour (H_2O). The observed patterns indicate the location of major sources. NO_2 is a pollutant which affects human health. HCHO is produced during the degradation of methane and by biomass burning. CO is produced by biomass burning, traffic and industrial processes. Water vapour is the most important natural greenhouse gas and is controlled by evaporation, transport and precipitation processes (Wagner et al., 2008).

3   BASICS OF ATMOSPHERIC RADIATION

Atmospheric radiation describes the interaction of solar and terrestrial radiation with molecules, aerosols, and cloud particles in planetary atmospheres, as well as with the surface. It is studied through the theory of radiative transfer and radiometric observations made from the ground, air and space. This field of study is closely related with the investigation of the atmospheric composition and atmospheric greenhouse effect.

The properties of electromagnetic radiation interacting with matter are systematized in a set of rules called radiation laws. These laws apply when the radiating body is what physicists call a blackbody. Generally, black body conditions apply when the radiator has very weak interaction with the surrounding environment and can be considered to be in a state of thermal equilibrium. Although stars do not satisfy perfectly the conditions to be black bodies, they do to a sufficiently good extent to consider the Sun as an approximate blackbody radiator. Four radiation laws, Planck's, Stefan-Boltzmann, Wien's displacement and Kirchhoff's law, are outlined below.

In this chapter scattering and absorption are also presented, processes that attenuate the solar radiation and are therefore important for detection of atmospheric chemicals with spectroscopy. In addition, to understand how the footprints of trace gases are created, the absorption line formation is discussed with short description of Bohr's model of the atom.

This chapter is based on K. N. Liou's book An Introduction to Atmospheric Radiation (Liou, 2002). It has been supplemented with material from other sources (Oštir, 2006, http://feps.as.arizona.edu/, Physics 2000).

3.1   Electromagnetic spectrum

Electromagnetic radiation is the most important process responsible for energy transfer in the atmosphere. It travels in wave form, and all electromagnetic waves travel with the same speed, the speed of light. The speed of light in the vacuum is c_0 = 299 792 458 m/s ≈ 300 000 km/s and very nearly the same speed in the air. Electromagnetic radiation is described with wavelength (λ), frequency (ν), and amplitude (A). Wavelength is the distance between two points with the same phase (e.g. two peaks of the waves), while the frequency refers to the number of oscillations in one unit of time. Wavelength λ and frequency ν are connected via speed of EM radiation:

$$c = \lambda \, \nu \qquad\qquad (1).$$

The whole series of all wavelengths (frequencies), from gamma rays, x-rays, ultraviolet light, visible light to infrared radiation, microwaves and radio waves constitute the electromagnetic spectrum. This term refers to the radiation range that is being emitted or reflected by a certain body.
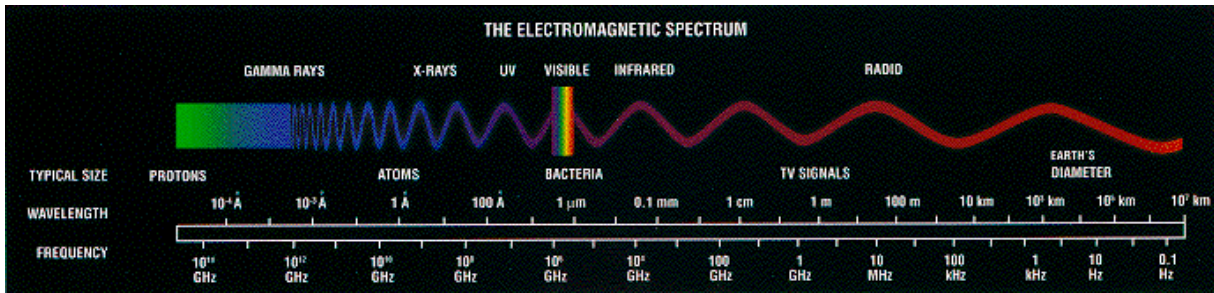
Figure 11: Electromagnetic spectrum

Gamma rays and X-rays have relatively short wavelengths, while infrared and radio waves have relatively long wavelengths. Visible light exists somewhere in the middle and it spans a very small portion of the spectrum.

Because visible light is one of the few types of radiation that can penetrate our atmosphere, our eyes naturally evolved to detect it. The Earth's atmosphere actually blocks out most of the electromagnetic spectrum. It only allows certain wavelengths to pass through. Ozone and ordinary oxygen completely block gamma and x-rays. Also ultraviolet radiation's short wavelengths are absorbed in higher atmosphere by ozone. Infrared radiation is mostly absorbed by water vapour and carbon dioxide, though there are specific wavelengths in infrared and in microwaves that can reach the surface. Very long wavelengths ($\lambda > 10$ m) are blocked by electric charges in the upper atmosphere.

Table 2: Electromagnetic spectrum used in remote sensing.

Electromagnetic spectrum	
Ultraviolet	$\lambda < 0.4$ μm
Visible light	$\lambda = 0.4$ to 0.7 μm
Near IR	$\lambda = 0.7$ to 1.35 μm
Middle IR (SWIR)	$\lambda = 1.35$ to 3.0 μm
Thermal IR	$\lambda = 3.0$ to 14.0 μm
Microwave	$\lambda = 1$ mm to 1 m
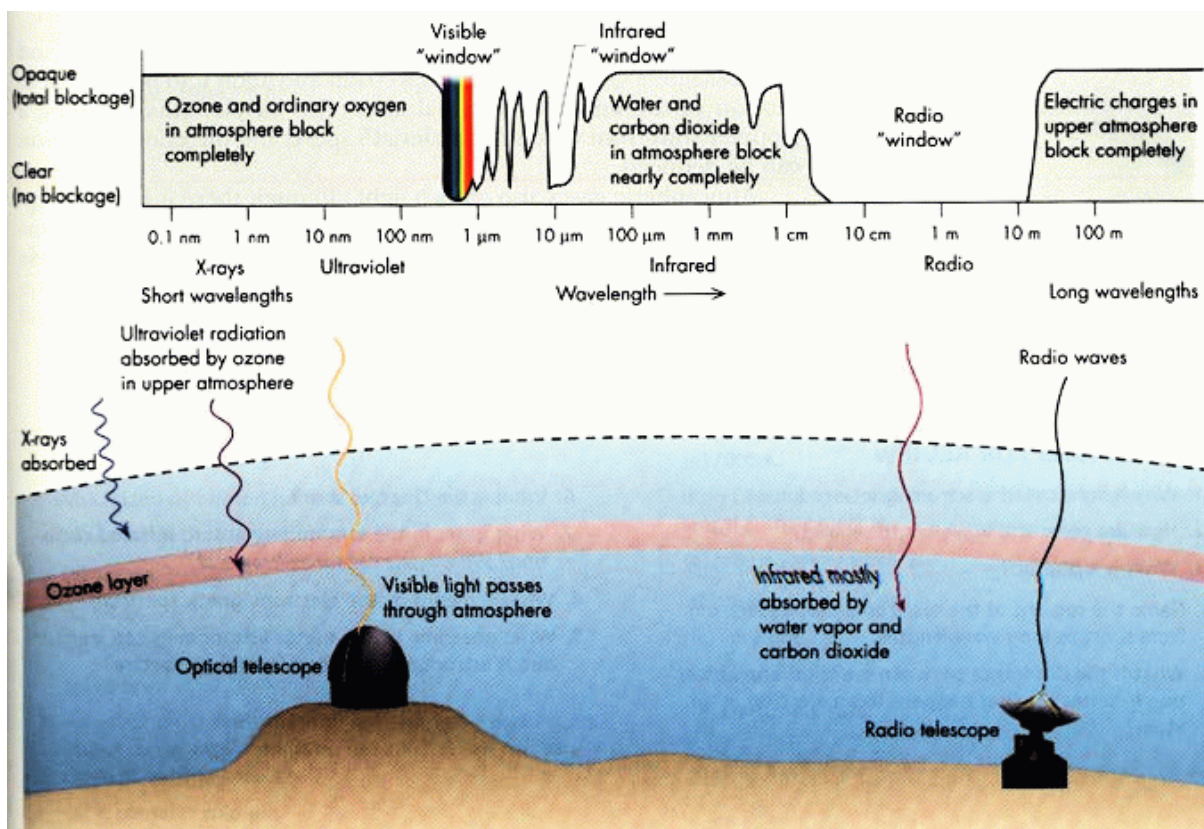
Figure 12: Atmospheric windows in the electromagnetic spectrum (http://feps.as.arizona.edu/, 8.12.2010).

3.2 Basic radiometric quantities

Radiometry studies the measurement of electromagnetic radiation. It deals with the measurement of energy per time - power, thus, the units of all radiometric quantities are based on joules per second or watts (W; 1 W = 1 J/s).

Light is a radiant energy. Electromagnetic radiation transports energy through space. Radiant energy (denoted as Q) is measured in joules (J; 1 J = 1 Nm).

Some light sources such as the Sun emit electromagnetic radiation in most of the electromagnetic spectrum. Lasers, on the other hand, are monochromatic sources – all of the radiant energy is emitted at one specific wavelength. We can define spectral radiant energy, which is the amount of radiant energy per unit wavelength interval at wavelength λ, as:

$$Q_\lambda = \frac{dQ}{d\lambda} \tag{2}$$

Spectral radiant energy is given in joules per nanometre (J/nm).

Another important radiometric quantity is radiant flux or radiant power, which is commonly referred to as *time rate of flow of radiant energy* and is defined as:

$$\Phi = \frac{dQ}{dt}$$

(3),

where Q is radiant energy and t is time. Radiant flux is measured in watts. Analogous to electric current, radiant flux is directly proportional to instantaneous electric current while the radiant energy corresponds to the total amount of current measured over a period of time.

Spectral radiant flux is radiant flux per unit wavelength interval at wavelength λ. It is defined as:

$$\Phi_\lambda = \frac{d\Phi}{d\lambda}$$

(4)

and is measured in watts per nanometre.

Radiant flux density is the radiant flux per unit area at a point on a surface. The flux can be arriving at the surface, in which case the radiant flux density is referred to as irradiance, or the flux can arrive from any direction above the surface. Irradiance is defined as:

$$E = \frac{d\Phi}{dA}$$

(5),

where Φ is the radiant flux arriving at the point and dA is the differential area surrounding the point. If the flux is leaving the point due to emission and/or reflectance, the radiant flux is referred to as radiant emittance:

$$M = \frac{d\Phi}{dA}$$

(6),

where Φ is the radiant flux leaving the point and dA is the differential area surrounding the point. Radiant flux density is measured in watts per square metre.

Figure 13: Irradiance (left) is the electromagnetic radiation incident on the surface. Radiant emittance (right) is a term describing the radiation that is emerging from the surface. Irradiance and radiant emittance are radiometry terms for the power of electromagnetic radiation per unit area at a surface. The SI unit for both quantities are watts per square metre (W/m^2).

Spectral radiant flux density is radiant flux density per unit wavelength interval at wavelength λ and is measured in watts per square metre per nanometre.

Radiance and spectral radiance are radiometric measures that describe the amount of light that passes through or is emitted from a particular area, and falls within a given solid angle in a specified direction. The SI unit of radiance is watts per steradian per square metre (W·sr^{-1}·m^{-2}). Radiance is defined as:

$$L = \frac{d^2\Phi}{dA(d\omega\cos\theta)}$$

(7),

where Φ is the radiant flux, dA is the differential area surrounding the point, $d\omega$ is the differential solid angle of the elemental cone, and θ is the angle between the ray and the surface normal n at the point (Ashdown, 2002).
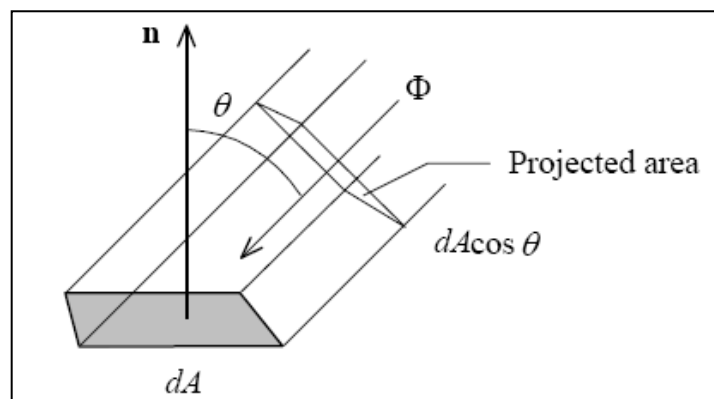
Figure 14: A ray of light intersecting the surface.

Table 3: SI radiometric units (Wikipedia, 9.12.2010)

Quantity	Symbol	SI unit	Abbr.	Notes
Radiant energy	Q	joule	J	Energy
Radiant flux	Φ	watt	W	Radiant energy per unit time, also called radiant power
Radiant flux density	j	watt per square metre	$W \cdot m^{-2}$	Radiant flux per square metre
Radiant intensity	I	watt per steradian	$W \cdot sr^{-1}$	Power per unit solid angle
Radiance	L	watt per steradian per square metre	$W \cdot sr^{-1} \cdot m^{-2}$	Power per unit solid angle per unit projected source area
Irradiance	E, I	watt per square metre	$W \cdot m^{-2}$	Power incident on a surface
Radiant emmitance	M	watt per square metre	$W \cdot m^{-2}$	Power emitted from a surface
Spectral radiance	L_λ	watt per steradian per metre³	$W \cdot sr^{-1} \cdot m^{-3}$	Commonly measured in $W \cdot sr{-1} \cdot m{-2} \cdot nm{-1}$
Spectral irradiance	E_λ	watt per metre³	$W \cdot m^{-3}$	Commonly measured in $W \cdot m{-2} \cdot nm{-1}$

3.3   Blackbody radiation laws

A black body is defined as an object that completely absorbs electromagnetic radiation that falls on it, and emits EM radiation in a wavelength spectrum determined solely by its temperature. This thermal radiation from a blackbody is termed blackbody radiation. The higher the temperature of the blackbody is, the higher the frequency of its radiation, and the shorter its wavelength. Emission and absorption reach an equilibrium condition with respect to the temperature. In the following, the four fundamental laws that govern blackbody radiation are presented.

Sun and Earth are not perfect black bodies but are sufficiently good approximation that blackbody radiation laws can be applied yielding useful results.

3.3.1   Planck's law

Planck's law describes the electromagnetic radiation emitted from a black body at absolute temperature T – how much radiation at certain wavelength the body emits at certain temperature. The Planck's function relates the emitted monochromatic intensity to the frequency and the temperature of the emitting substance.

$$B_\lambda(T) = \frac{2hc^2}{\lambda^5\left(e^{hc/\kappa\lambda T} - 1\right)}$$

(8),

where K is Boltzmann's constant, c is the velocity of light, T is the absolute temperature and h is Planck's constant.

Planck's law states that the energy of electromagnetic radiation is confined to indivisible packets (quanta), each of which has energy equal to the product of the Planck constant and the frequency of the radiation. This law is the basis of quantum theory, the theoretical basis of modern physics.

3.3.2   Stefan – Boltzmann law

Stefan-Boltzmann law is fundamental to the analysis of broadband infrared radiative transfer. It states that the flux density (j) emitted by a blackbody is proportional to the fourth power of the absolute temperature (T) of the body.

$$j = \pi B(T) = \sigma T^4$$

(9),

where $B(T)$ is total radiant intensity of a blackbody derived by integrating the Planck function over the entire wavelength domain from 0 to ∞ and $\sigma = 5.670373 \times 10^{-8}$ W m^{-2} K^{-4} is the Stefan-Boltzmann constant. This law is named after Jožef Stefan[1] (1835 – 1893) and is the only law of physics that is

---

[1] Jožef Stefan (1835 – 1893) was one of the most important physicists of 19th century. He was investigating mechanics, optics, magnetism and electricity. He is best known for originating a physical power law in 1879 – Stefan-Boltzmann Law.

He was born in Slovenian family near Klagenfurt (Celovec) in Austria-Hungary (now Austria). His father worked as a miller of flour and as a baker, his mother was employed as a maidservant. Stefan graduated in physics and mathematics at the University of Vienna in 1857. During his student years he wrote and published a number of patriotic and romantic poems in Slovene. He taught physics at the University of Vienna, was Director of the Physical Institute from 1866, Vice-President of the Vienna Academy of Sciences and member of several scientific institutions in Europe. He died in Vienna in 1893. The Jožef Stefan Institute, the largest research institution in Slovenia, as well as one of the lunar craters are named after him (Wikipedia, 25.6.2011).

named after Slovenian physicist. With his law Stefan determined the temperature of the Sun's surface and he calculated a value of 5430 °C. This was the first sensible value for the temperature of the Sun.
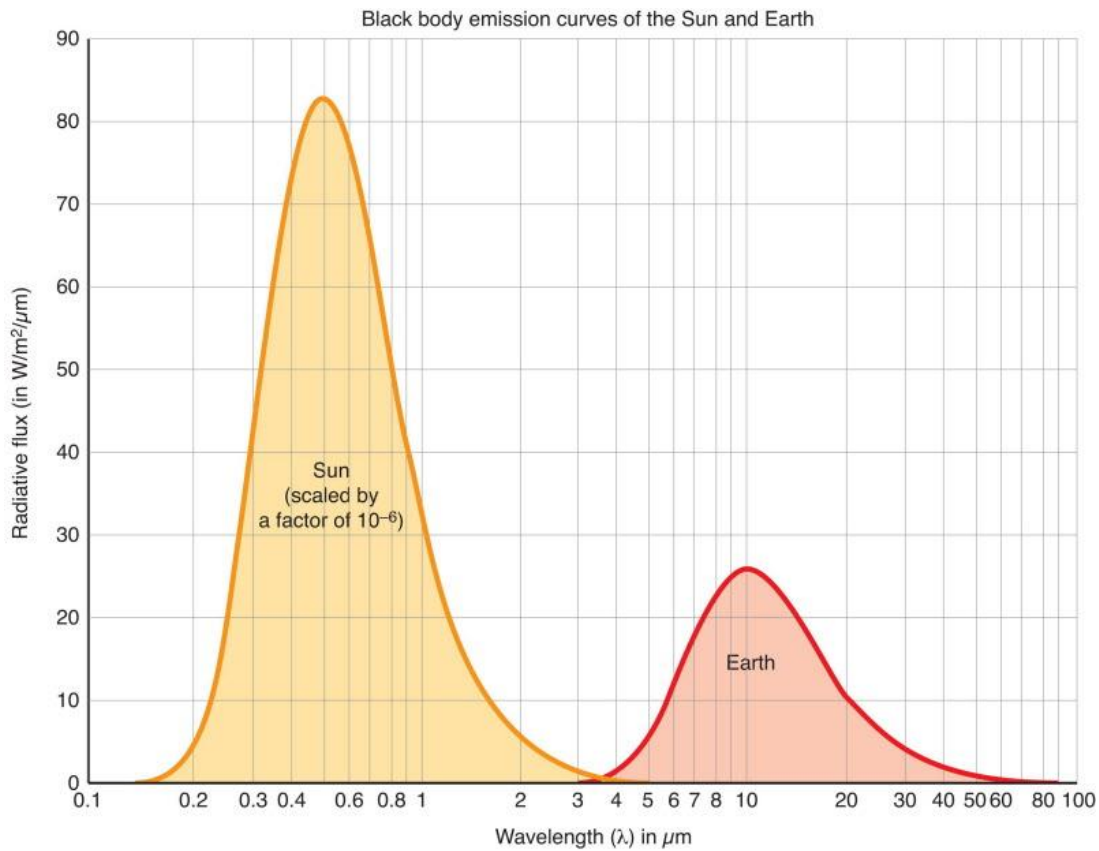
Figure 15: Blackbody emission curves of the Sun (6000 K) and Earth (288 K) (The Science of Doom, 2010).

3.3.3 Wien's displacement law

According to Wien's law, the wavelength of the maximum intensity of the blackbody radiation is inversely proportional to the temperature:

$$\lambda_{\max} = {a}\!/\!{T}$$

(10),

where a = 2 897 768.5 nm K (a constant). We obtain the wavelength of the maximum by differentiating the Planck function with respect to wavelength and setting the result equal to zero. The wavelength of the maximum gets shorter if the temperature increases. From Wien's relationship we can determinate the temperature of a blackbody from a measurement of the maximum monochromatic intensity.

Table 4: Temperatures and characteristic wavelengths. The table summarizes blackbody temperatures necessary to give a peak of emitted radiation in various reigns of the spectrum. All heated objects emit a characteristic spectrum of electromagnetic radiation and this spectrum is concentrated in higher wavelengths for cooler bodies.

Some Blackbody Temperatures			
Region	Wavelength (cm)	Energy (eV)	Blackbody Temperature (K)
Radio	> 10	< 10^{-5}	< 0.03
Microwave	10 – 0.01	10^{-5} – 0.01	0.03 – 30
Infrared	0.01 – 7 10^{-5}	0.01 – 2	30 – 4100
Visible	7 10^{-5} – 4 10^{-5}	2 – 3	4100 – 7300
Ultraviolet	4 10^{-5} – 10^{-7}	3 – 10^3	7300 – 3 x 10^6
X-Rays	10^{-7} – 10^{-9}	10^3 – 10^5	3 x 10^6 – 3 x 10^8
Gamma Rays	< 10^{-9}	> 10^5	> 3 x 10^8

The Wien law gives the wavelength of the position of the maximum (peak) of the radiation distribution, while the Stefan-Boltzmann law gives the total energy being emitted at all wavelengths by the blackbody (which is the area under the Planck law curve, see Figure 15). Thus, the Wien law explains the shift of the peak to shorter wavelengths as the temperature increases, while the Stefan-Boltzmann law explains the growth in the height of the curve as the temperature increases. The growth varies as the fourth power of the temperature (Cartage, 2011).

3.3.4 Kirchhoff's law

The concept of the blackbody is an idealisation – a real body will emit less radiation than the ideal black one. The ratio of the spectral radiance from that body to the spectral radiance from a blackbody is called the spectral emittance ε_v of a body. The blackbody emits the maximum possible amount of energy in each frequency interval at a given temperature, therefore $\varepsilon_v \leq 1$. We can also define the spectral absorptance α_v as the fraction of energy per unit frequency interval falling on a body that is absorbed. Kirchhoff's law states that at a given temperature and frequency the spectral emittance of a body equals its spectral absorptance:

$$\varepsilon_v = \alpha_v$$

(11).

3.4   Scattering and absorption

Most of the light we see does not come directly from its source but indirectly through the process of scattering. The sunlight is scattered by the particles in the atmosphere, the electric light is scattered by the glass bulb. Unless we look directly at a light source, such as the Sun or an incandescent filament with a clear bulb, we see light that has been scattered. Blue sky, rainbows and auroras are also the result of light scattering[2]. Also the objects surrounding us are visible through the light that they scatter.

Scattering is a physical process by which a particle in the part of an electromagnetic wave continuously abstracts energy from the incident wave and reradiates that energy in all directions. In the atmosphere, the particles responsible for scattering range in size from gas molecules ($\sim10^{-4}$ μm) to aerosols (~1 μm), water droplets (~10 μm), ice crystals (~100 μm), and large raindrops and hail particles (~1 cm). The scattering way is dependent on the ratio of the particle circumference to the incident wavelength λ, i.e. $x = 2\pi a/\lambda$, where a is a particle radius. If $x \ll 1$, Rayleigh scattering is predominant. An example of this case is the scattering of visible light ($0.4 - 0.7$ μm) by atmospheric molecules, leading to the blue sky. When the size of the particles is comparable or larger than the wavelength, i.e. $x \approx > 1$, Lorenz-Mie scattering is the most important.

In Rayleigh and Lorenz-Mie scattering the kinetic energy of the incident particles is conserved by the interaction with other particles, only their direction of propagation is modified. Such scattering is called elastic scattering. Inelastic scattering, on the other hand, refers to scattering, when total kinetic energy is not conserved; some of the energy of the incident energy is lost or gained. Inelastic scattering is called Raman scattering (Wikipedia, 26.6.2011)

---

[2] Sunlight that reaches Earth's atmosphere is scattered in all directions by all the gases and particles in the air. Molecules in the air are much smaller than the wavelength of the light therefore Rayleigh scattering is predominant. Rayleigh scattering is inversely proportional to the fourth power of wavelength, so shorter wavelength blue light (420 nm) scatters much more than the longer wavelength red light (750 nm). The longer the light's path through gas the more blue light is scattered and the more red becomes the beam. That is why the Sun high in the sky looks yellow and red at sunset (at horizon the path through atmosphere is longer).

The rainbow appears in the sky when it is raining and the Sun is shining on the rain clouds. It is a consequence of refraction and reflection of sunlight on the raindrops. Raindrops act as prisms – they divide the white light into its one-colour components. Different wavelengths are refracted under a different angle.
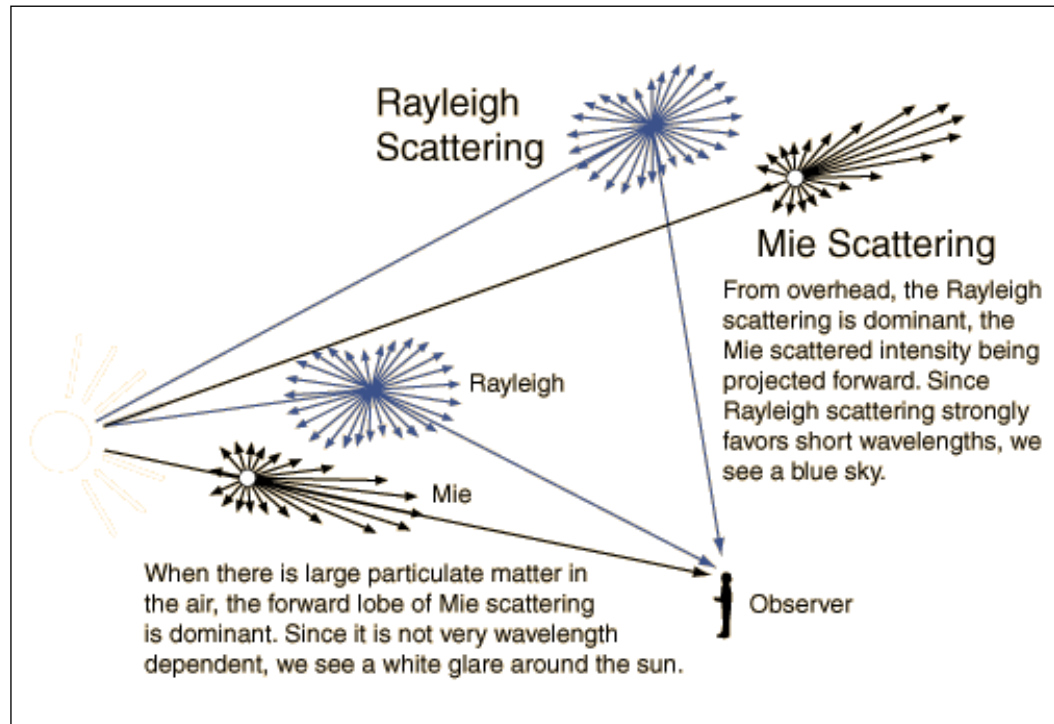
Figure 16: Rayleigh scattering and Mie scattering description (GSU, 2011).

Scattering is often accompanied by absorption. Usually it is the combined effect of scattering and absorption to give objects their colours: grass looks green because it scatters the green light while it absorbs red and blue light. In molecular atmospheres there is very little absorption in visible light. Both scattering and absorption remove energy from a beam of light traversing the medium. The different molecules in the atmosphere absorb radiation of different wavelengths. The absorption spectrum will show a number of bands corresponding to different molecules. By looking into absorption spectrum, we can extract information about the abundance of different species in the atmosphere.
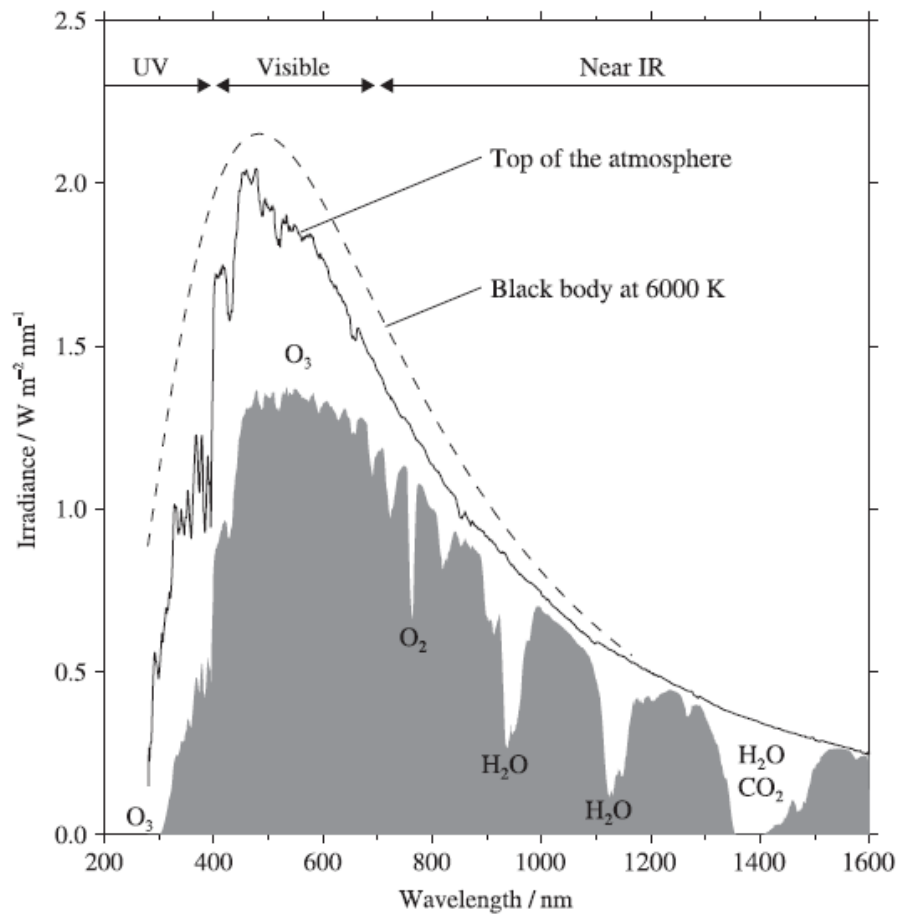
Figure 17: The irradiance spectrum of solar radiation at the top of the atmosphere (solid line) and at sea level (shaded), compared with the black-body irradiance spectrum (dashed line) for T=6000 K. (Andrews, 2010, page 71)

3.5   Absorption line formation and line shape

3.5.1   Spectral lines

The vibration of electrons inside atoms gives off light and other electromagnetic radiations. If we direct the sunlight through the prism we see the whole rainbow because the prism breaks the light into all of its separate colours. But when we look at the light coming off of just one element, hydrogen for instance, not the whole spectrum can be seen. Instead there are just bright lines of certain colours. That means that the atoms are only emitting waves of certain frequencies. Each type of atom gives off a unique set of colours. These lines are called spectral lines or Fraunhofer lines and are a kind of a signature for the atoms. The science using spectral lines to figure out what something is made of is spectroscopy. That is how we know the composition of distant stars, for instance (NFSI, 2010).
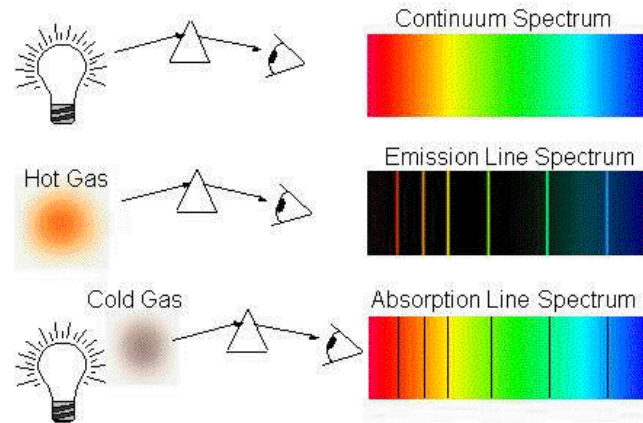
Figure 18: Continuum spectrum and emission and absorption spectrum (Smith, 2009).

Normally the lines we see are not as pure as they should be according to theory. Due to different influences the loss in energy occurs during energy transition and as a consequence emitted radiation is non-monochromatic – the observed spectral lines are broader. The broadening of spectral lines is caused by: (1) the damping of oscillator vibrations resulting from the loss of energy in emission (normal broadening); (2) the collisions between molecules (pressure broadening); and (3) the Doppler effect resulting from the difference in thermal velocities of atoms and molecules.

3.5.2   Bohr's model

To explain the spectral lines, Bohr (1913) provided a radical model of atom with electrons orbiting around a nucleus. Electrons can only be in "special" orbits but they can jump between these orbits, however, and when they jump this cause radiation. Each time the electrons jump from one orbit to another, little burst of light (electromagnetic energy), called photon, emits. Energy can only change in little jumps – quanta. Radiation occurs only when atom makes a transition from the state with energy E_k to a state with lower energy (electron jumps from one orbit to another, which is closer to the nucleus) E_j:

$$E_k - E_j = h\nu$$

(12),

where $h\nu$ is a quantum of energy carried by the photon, which is emitted from the atom during the transition. When an electron of atom due to a collision jumps into a larger orbit, it absorbs energy. Each quantum jump between fixed energy level results in the emission or absorption of a characteristic frequency or wavelength emission or absorption spectral lines (Physics 2000, 2010).

To summarize the chapter, the Sun is the most obvious source of EM radiation for remote sensing, but all objects at temperatures above absolute zero (0 K or -273°C) continuously emit EM radiation. The amount of energy emitted is a function of the objects surface temperature as set forth in the Stefan-Boltzmann law. The spectral distribution of emitted energy varies with temperature according to Wien's Displacement law.

Together, the Stefan-Boltzmann law and Wien's law stipulate that:

- the higher the temperature of a radiator, the greatest the amount of radiation it emits (area under the curve on Figure 15)
- as temperature increases, the peak of the spectral radiation distribution shifts toward shorter wavelengths

4   OPTICAL INSTRUMENTS FOR GAS CONCENTRATION DETECTION

This chapter deals with instruments for detection of atmospheric gases that are based on spectroscopy. Space-based spectrometers split the light passing through the atmosphere into visible and invisible individual wavelengths to look for distinctive absorption or emission 'footprints' left by global warming chemicals. The principals of spectroscopy as well as basic characteristics of spectrometers including the quality parameters and possible error sources are presented. As one of the most commonly used and very effective technique for trace gas total column retrieval the differential optical absorption spectrometry (DOAS) is described.

4.1   Spectroscopy

Spectroscopy is the study of electromagnetic spectra – the wavelength composition of light – due to atomic and molecular interactions. Spectroscopy is very important in the study of physics as well as in astronomical, biological, chemical, metallurgical and other analytical investigations. It is used as a detector of atomic species to determine the characteristics of celestial bodies and the presence of atmospheres in the planets, to identify unknown compounds, to study the structures of molecules and atoms and much more. In astrophysics, diffraction gratings provide clues to the composition of and processes in stars and planetary atmospheres, as well as offer clues to the large-scale motions of objects in the universe. In chemistry, toxicology and forensic science, grating-based instruments are used to determine the presence and concentration of chemical species in samples.

4.2   Spectrometer

Spectrometer, also known as spectrograph, spectrophotometer or spectroscope is a major tool used by scientists to gather information about the universe, galaxies, stars and planets. It is an instrument that has made exploration of faraway light sources possible and helped us understand the composition of stars including our Sun.

Spectrometer is used to analyze the nature of light emitted by various sources. It is a measuring device that collects light waves and splits the incoming light into its component colours creating a frequency spectrum.

Before the radiation reaches the spectrometer, it goes through the telescope. The focal point of the telescope beam is brought to the slit of the spectrometer, a narrow aperture through which the radiation from the Earth enters the spectroscope. This slit is what is ultimately imaged on the detector. The light passing through the slit is reflected off a collimating mirror, which parallelizes the beam of light, before sending it off to the diffraction grating. This optical element disperses the parallel beams of light into their component colours/wavelengths/energies. Each different wavelength comes off of the grating at a slightly different angle. So now, we have an image of the slit that is spread out like a

rainbow by colour. This new colour-dispersed beam of light is then focused and imaged on the detector.
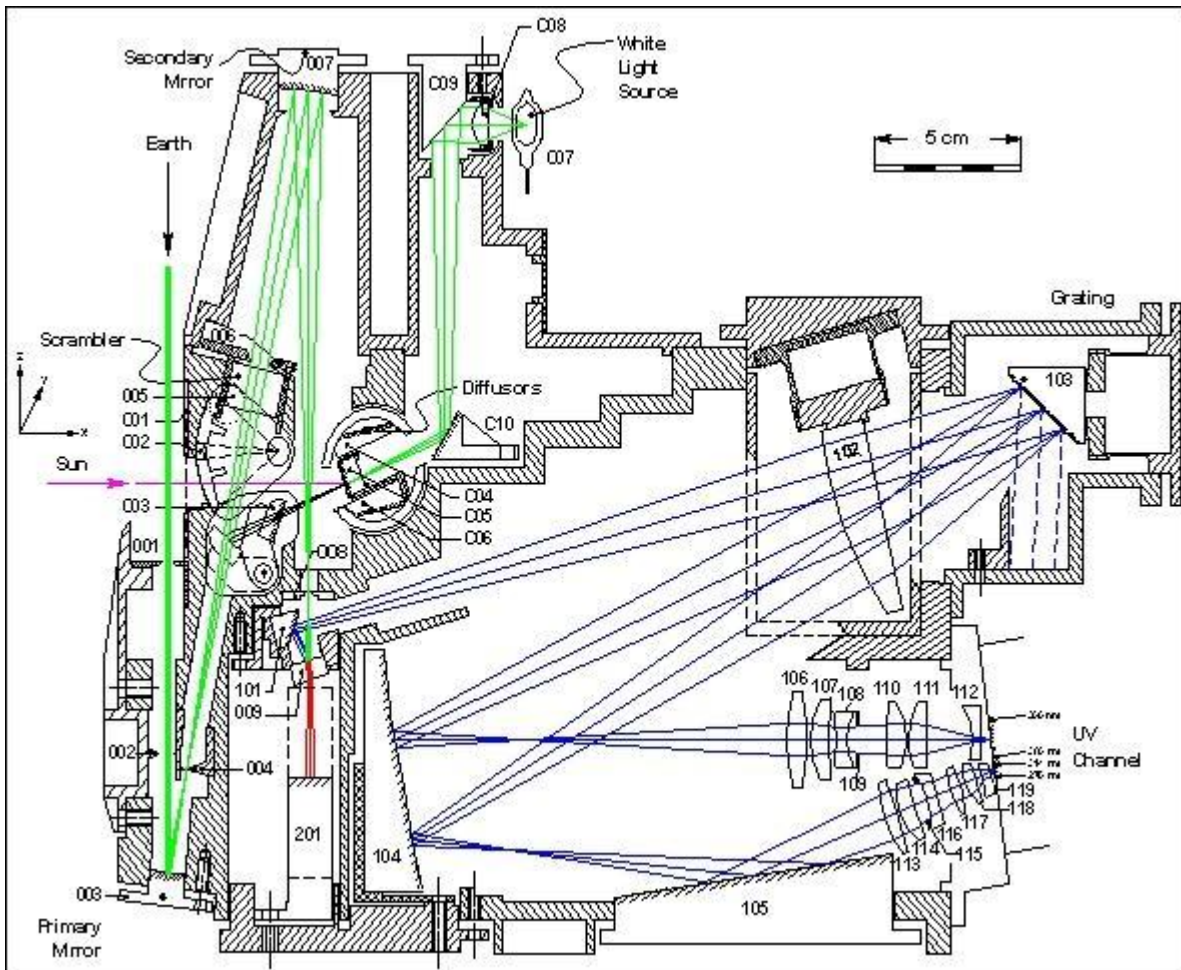
Figure 19: Optical design of UV channel of OMI instrument (OMI, 2011).

CCD (Charged Coupled Device) reads the intensity of the various light components and converts them into electronic signals. The image of one-dimensional slit on the detector is two-dimensional: rows are representing the slit and in columns there are different wavelengths of the light corresponding to each part of the slit. Because the light is dispersed all over the detector the effective brightness of an object on the detector is much lower than when taking images of an object. This means that it takes a bigger telescope and/or longer integration time to get a good spectrum than an image.

The broader the light is dispersed and the narrower the slit is, the better spectral resolution; one can see finer and more subtle features in the spectrum.
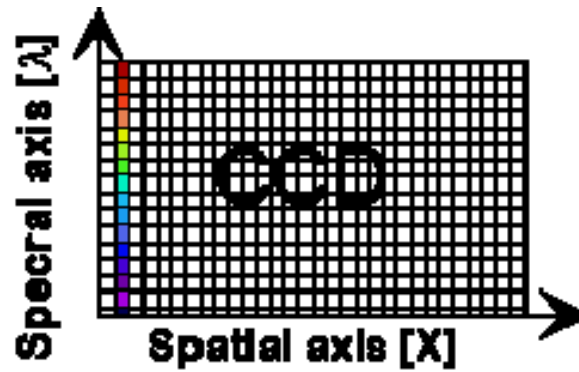
Figure 20: Spatial and spectral representation of the dispersed object line depicted onto the CCD matrix detector. Spatial axis X represents the image of the slit in one exposure. Each column corresponds to one spatial pixel and describes the intensity of each narrow wavelength band that was detected in this picture. Each pixel of the CCD camera, therefore, measures the light intensity according to the spatial position and spectral location. Each exposure generates one λx plane. Moving of the payload in y-axes direction perpendicular to λx plane gives us 3-dimentional data.

4.2.1   Spectrometer's parameters

Spectrometer's parameters are the basic characteristics defining its quality. There are many parameters, most important are outlined below.

Spectrometers operate in a very wide *wavelength range*, from gamma rays and X-rays into the far infrared. However, because of the different techniques used to measure different portions of the spectrum, any particular instrument will operate over a small portion of this total range. By the wavelength range in connection with desired spectral resolution the size of the spectrograph is determined.

Spectral resolution indicates how well the sensor provides different wavelengths. The better the spectral resolution is, the narrower are the spectral bands (channels) and the more of them are present. The spectral resolution is determined by the width of the input slit, the focal length of the optical system and the dispersion of the grating. The smaller the slit width, the higher is the resolution. Spectral resolution is usually defined by

$$R = \frac{\lambda}{\Delta\lambda} \tag{13},$$

where $\Delta\lambda$ is the smallest difference in wavelengths that can be distinguished, at a wavelength of λ.

When an image is created its *radiometric resolution* is defined by the sensitivity to the intensity of the electromagnetic radiation. Radiometric resolution tells us how well the system can differentiate between small differences in the energy of radiation, and is usually expressed as a number of levels or a number of bits, for example 8 bits or 256 levels, which is typical of computer image files. The higher the radiometric resolution, the better subtle differences of intensity or reflectivity can be represented, at least in theory. In practice, the effective radiometric resolution is typically limited by the noise level, rather than by the number of bits of representation.

In optics *distortion* is a type of aberration, in which there is variation of magnification with the distance from the axis of an optical system, so that images are not geometrically similar to their objects – the images of the slit in different wavelength are not completely straight and parallel. The most problematic distortions are the keystone effect and smile effect. Smile is a change in dispersion with field position, and spectral keystone is a change in magnification with wavelength. Spectral keystone involves mixing of spectra from adjacent field positions (Fischer et al., 1998).
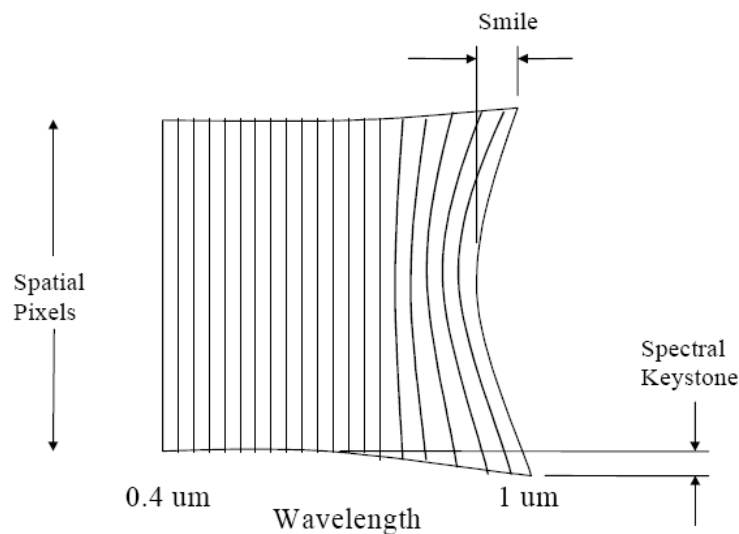
Figure 21: Definition of smile and keystone effect (Fischer et al., 1998).

Quantum efficiency (QE) is a quantity defined for a photosensitive device such as photographic film or a charge-coupled device (CCD) as the percentage of photons hitting the photo-reactive surface that will produce an electron–hole pair. It is an accurate measurement of the device's electrical sensitivity to light. Since the energy of a photon depends on (more precisely, is inversely proportional to) its wavelength, QE is often measured over a range of different wavelengths to characterize a device's efficiency at each photon energy. It is normally expressed in percentage. Photographic film typically

has a QE of much less than 10%, while CCDs can have a QE of well over 90% at some wavelengths. (Wikipedia, 25.2.2011)
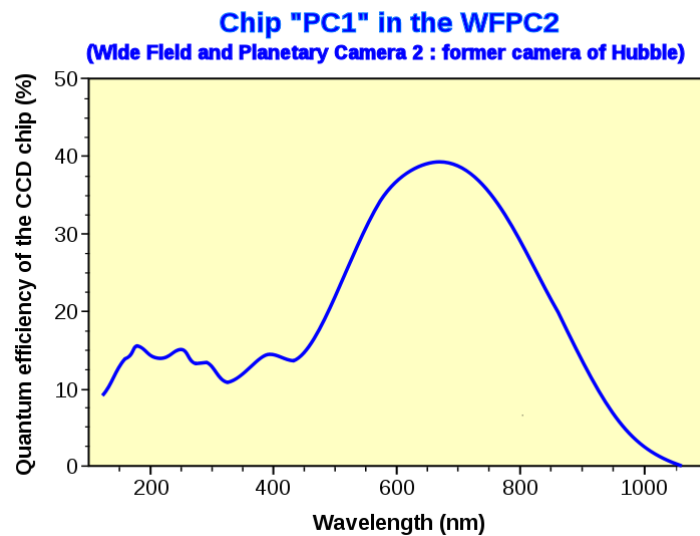
Figure 22: A graph showing variation of quantum efficiency with wavelength of a CCD chip in the Hubble Space Telescope's Wide Field and Planetary Camera 2. (Wikipedia, 25.2.2011)

4.2.2   Error sources

Like any remote sensing technique, also spectroscopic retrieval of atmospheric gases is susceptible to three types of error sources:

- forward model errors,
- inverse model errors, and
- instrumental errors.

Forward model errors include errors that occur in the computation of radiances. Scattering and absorption in the atmosphere, as well as effects of clouds, aerosols and surfaces on electromagnetic radiation are complex processes and even the best radiative transfer model cannot approximate it without errors. Under normal circumstances, those errors usually contribute less than 1% RMS error in the computation of gas total column. In some use cases, e.g. in determining long-term trend from a particular type of instrument, those errors are unimportant, but they are very important when comparing two different systems (Bhartia, 2002).

The *inverse model errors* are caused by the fact that the inversion of radiances into geophysical parameters requires a priori information on how the gas under consideration is distributed vertically in the atmosphere in order to correct for the effects of atmospheric temperature and pressure. Errors in a priori introduce also retrieval errors, but those are usually quite small, below 1% (Bhartia, 2002).

36   Urbas, A. 2011. Effects of instrumental errors in the retrieval of anthropogenic gas distribution from satellite.

Grad. Th. – University Studies. Ljubljana, UL FGG, Department of Geodetic Engineering.

Instrumental errors, on the other hand, have considerably bigger effect on the trace gas retrieval accuracy. The most important instrumental errors are instrumental noise, stray light and spectral mis-registration. The effect of those three error sources have been assessed in the simulations of NO_2 retrieval with TROPOMI instrument and the results are presented in chapter 7.

a. Stray light

Stray light is an unwanted scattered radiation of false wavelength within an instrument, which strikes a pixel. It is caused by imperfections of the grating, dust, reflexion of the spectrometer housing or errors of other optical elements. It is often the major source of measurement uncertainty for commonly used spectrometers. There are two types of stray light, the spectral stray light and the spatial stray light. Spectral stay light is light of a certain wavelength, which is scattered to a detector pixel 'belonging' to a different wavelength. It can lead to distortions in the shape of the spectrum. This type of the stray light is usually caused by a reflection in the instrument after the dispersion of a light beam. It is also called in-field stray light. Spatial stray, also called out-of-field stray light, is light entering the telescope but coming from the bright sources outside of instantaneous field of view (IFoV) of the instrument as for example the Sun or the Moon. To reduce this effect telescopes are equipped with proper baffling systems composed by an external baffle and several light traps placed between the mirrors and close to the focal planes.

b. Noise

Noise is unwanted signal, which degrades the quality of the CCD image. It is random and cannot be completely removed from the image. There are three types of noise: dark current, readout noise and shot noise. Dark current noise is thermally generated – additional electrons are generated within the CCD not only by the absorption of photons (i.e. signal) but by physical processes within the CCD itself. The number of electrons generated in a second depends on the operating temperature of the sensor. Dark current has Poisson distribution (Mullard Space Science Laboratory, 2011). With sufficient cooling, dark current can be made negligible (Jørgensen 2002). Shot noise or photon noise produces a temporal variation in the output signal that is proportional to the square root of the signal level in electrons. Photon production is governed by the laws of quantum physics and has statistical nature therefore we cannot assume that, in a given pixel for two independent observation intervals of the same length, the same number of photons will be counted. The number of photons impinging on a CCD image sensor that generates charge carries is not exact, and it can only be described using probability. It follows the Poisson distribution (Jørgensen 2002). Noise electrons due to shot noise can be calculated with (14):

$$n_{shot} = \sqrt{\frac{\Phi}{h \cdot v} \cdot t \cdot A \cdot QE} = \sqrt{S} \qquad (14).$$

n_{shot} ... noise electrons due to shot noise

Φ ... light power [W/m^2]

$h \cdot v$ ... photon energy [Ws]

t ... exposure time [s]

A ... pixel area [m^2]

QE ... quantum efficiency

S ... detected signal

Readout noise is added during the conversion of the charge carries into a voltage signal, the subsequent processing and analogue-to-digital conversion. The noise is uniformly added to the image (PCO, 2010).

Total noise includes all three noise sources mentioned above. Since all of the three noise sources are not correlated, the total number of noise electrons is given by (PCO, 2010):

$$n_{total} = \sqrt{\left(\sqrt{\frac{\Phi}{h \cdot v} \cdot t \cdot A \cdot QE}\right)^2 + n_{dark}^2 + n_{readout}^2} \qquad (15).$$

n_{dark}^2 ... noise electrons due to dark current

$n_{readout}^2$ ... noise electrons due to readout noise

c. *Spectral mis-registration*

Spectral mis-registration is the error in wavelength knowledge. If detected signal is not exactly the wavelength it is believed to be, we consider this shift as spectral mis-registration. It can also be the result of smile effect – bending of spectral lines at the imaging plane. Spectral mis-registration error can be eliminated with spectral calibration.

4.3   Differential optical absorption spectroscopy (DOAS)

Differential optical absorption spectroscopy (DOAS) is a widely used reliable measurement technique for atmospheric trace gases probing. DOAS identifies and quantifies the trace gases in the atmosphere taking advantage of their molecular absorption structures in UV and visible wavelengths of the electromagnetic spectrum. In accordance with Palazzi (2008), this method was first used in late 70s by U. Platt and D. Perner. According to them, the main advantage of this technique over others is that it allows real-time measurements of several different trace-gas species with a single instrument. It can be used for ground based applications as well as satellite measurements, for both active and passive instruments. DOAS is the process whereby column densities of trace-species are derived from measurements of electromagnetic radiation in specified spectral intervals so that different trace species can be identified and separated. In the case of passive DOAS, which uses the Sun as radiation source, the trace gases absorption is analyzed and quantified to conclude on the concentration of the trace gases integrated along the optical path between the Sun and the receiver. Therefore the optical path of light collected by the system has to be well understood. (Palazzi, 2008, p. 18)

To perform DOAS, two spectra are necessary: one, referred to as the reference, in which the light has passed through little (ideally none) of the absorber in question and one, in which the light has passed through a large amount of the absorber. By comparing the spectra of the light source with and without the absorber in the light path, the integrated amount of the substance can be determined using Lambert-Beer's law. Depending on the absorption spectrum of the species of interest, light at ultraviolet, visible or short wave infrared (SWIR) wavelength can be used.

Lambert-Beer's law or Absorption law is the basic equation of absorption spectroscopy:

$$I(\lambda) = I_0(\lambda) e^{-L\sigma(\lambda)n} \tag{16},$$

where $I(\lambda)$ is the attenuated beam (after traversing the media), $I_0(\lambda)$ is the incident or reference beam, L the path length [cm], $\sigma(\lambda)$ the wavelength dependent absorption cross section [cm^2 / molecule], and n the number density of the species [molecules / cm^3]. The dimensionless quantity $L \cdot \sigma \cdot n$ is often referred to as the optical depth, denoted τ. This law involves no directional dependence, so it is applicable not only to the intensity quantity but also to the flux density and the flux.

In atmospheric conditions Rayleigh and Mie scattering also contribute to the radiation extinction. By scattering light away from the line of sight these phenomena acts like absorption processes, although they are actually not. Adding Rayleigh factor to (16) gives:

$$\tau(\lambda) = \ln\left(\frac{I_0(\lambda)}{I(\lambda)}\right) = L \cdot \left(\sigma(\lambda)n + \varepsilon^R(\lambda) + \varepsilon^M(\lambda)\right)$$

$$(17),$$

where $\varepsilon^R(\lambda)$ is the Rayleigh extinction coefficient, which is the product of the Rayleigh cross section, $\sigma^R(\lambda)$, and the number density of air, n_{air}. Similarly, the Mie extinction coefficient, $\varepsilon^M(\lambda)$, corresponds to $\sigma^M(\lambda)n_{air}$ (Brohede, 2002).

Once we have the spectra of light that traversed the atmosphere, we compare it to the reference spectra. Where there are deviations, the light has been absorbed. Individual absorbers can be identified through their characteristic variation of absorption with wavelength, their spectral fingerprints. Extinction by scattering and absorption on the ground, which also attenuate the beam but are not a matter of our interest, usually vary smoothly with wavelength and can be removed from the signal by applying high pass filters (Richter, 2006).

Scattered sunlight DOAS measurements yield the slant column density of the respective absorbers, that is, the trace gas concentration integrated along the light path. For the determination of vertical column density (the vertically integrated trace gas concentration), the radiative transfer modelling is necessary (Palazzi, 2008, p. 38).
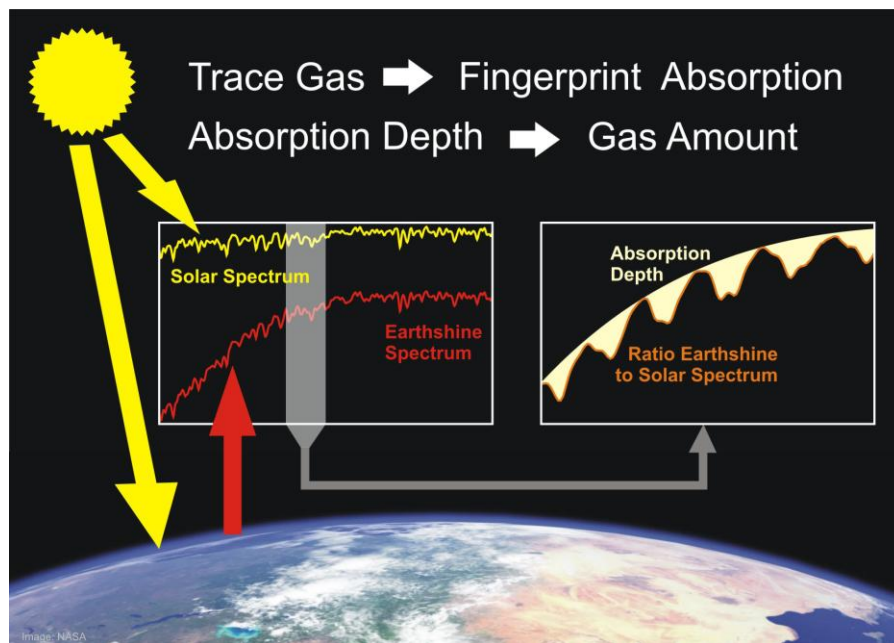
Figure 23: DOAS measurement principle (Kelder, 2008).

4.4   Retrieval of gas profiles

The outputs of the DOAS analysis are the slant column densities. In order to gain vertical column densities and profile information of the absorbers measured slant column densities have to be compared with model calculation. When modelling the radiative transfer in the atmosphere, a number of parameters have to be known. The most important ones are the viewing geometry, the position of the Sun, wavelength, and the vertical profiles of absorbers, pressure and temperature.

In DOAS the air mass factor is used to translate the slant column density into a vertical column density, which is independent of the viewing geometry. The air mass factor (AMF) M is defined as the ratio of the slant column density Ns and the vertical column density Nv.

$$M = \frac{N_s}{N_v}$$ (18).

The AMF depends on the Sun-satellite geometry, as well on the *state of the atmosphere*. With the latter it is meant that AMF depends on the trace gas profile, on clouds and aerosol properties, on surface reflectivity properties etc. (Bhartia, 2002).

The AMF can be determined using a radiative transfer model and an instrument simulator. The radiative transfer model produces radiances for a model atmosphere. The instrument simulator is used to produce spectra with the resolution and sampling of the instrument. We determine the slant column density by fitting DOAS to these spectra and divide by the known vertical column density to determine the air mass factor. The procedure to determine the air mass factor is schematically presented for the case of OMI instrument in the Figure 24.
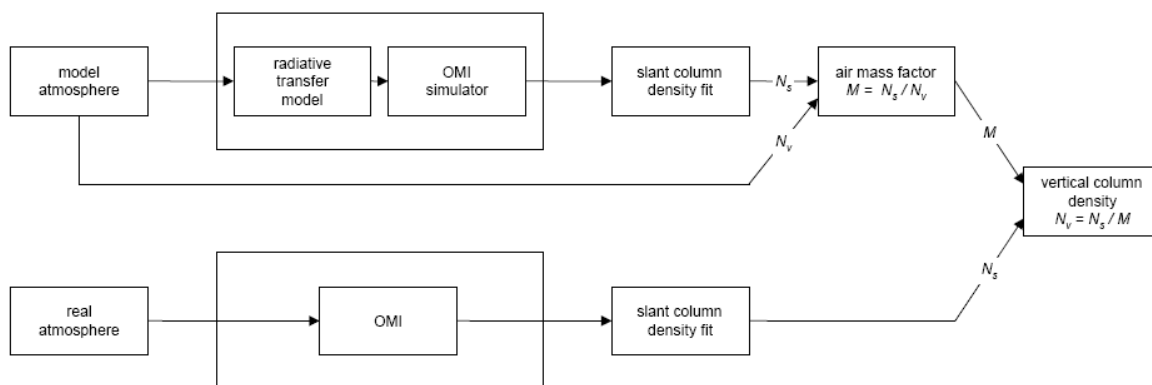
Figure 24: Schematic of the procedure to determine the air mass factor (Bhartia, 2002).

From vertical column density trace gas vertical profiles are obtained by comparing the data to the existing profiles.

5   OVERVIEW OF SPACE-BORNE INSTRUMENTS FOR TRACE GAS MEASUREMENTS

In this chapter space-borne instruments for trace gas detection that are based on the imaging spectroscopy are presented, shortly described and compared. Those instruments are GOME, SCIAMACHY, OMI and TROPOMI.

5.1   GOME

GOME stands for Global Ozone Monitoring Experiment. It is an instrument aboard the ERS-2 (European Remote Sensing) satellite, launched by the European Space Agency (ESA) in 1995. GOME is a spectrometer, which means that it measures Earthshine spectra: the sunlight, which is reflected back into space by molecules in the atmosphere and by the surface. The instrument also measures the solar spectrum directly. The ratio between the Earthshine and solar signal is a measure of the reflectivity of the Earth's atmosphere and surface (KNMI, 2011). GOME measures the spectra with four spectrometers simultaneously in a wide wavelength range, from the ultraviolet (240 nm), via the visible into the near-infrared (790 nm), at moderate spectral resolution of 0.2-0.4 nm. The satellite operates in a nearly polar, Sun-synchronous orbit at an altitude of 780 km. GOME instrument scans the surface in the perpendicular, east-west direction. Each sweep consists of three adjacent pixels, each covering an area of 320 km (east – west) by 40 km (north – south). The Earth's surface is totally covered within 3 days (Wagner et al., 2008).

From the measurement information, ozone and several other trace gas species in the atmosphere can be extracted. The primary function of GOME is monitoring ozone but the spectra it measures also give the information on other atmospheric species, such as the total concentration of nitrogen-dioxide, bromine and chlorine species, formaldehyde, sulphur-dioxide and the abundance of aerosols (particles) in the atmosphere.

GOME's mission ended after 16 years in September 2011 by decommissioning ERS-2 satellite[3].

In October 2006 GOME-2 instrument was launched onboard ESA's Meteorological Operational (MetOp) satellite. It is similar to the GOME instrument, but with finer spatial resolution (40×80 km^2) and almost global coverage (Wagner et al., 2008).

---

[3] Once placed in its final orbit at around 570 km altitude, the ERS-2 has been "passivated" (the batteries were disconnected and the communication system was switched off once all the fuel was depleted) (ESA, 2011).

5.2   SCIAMACHY

SCIAMACHY (SCanning Imaging Absorption spectroMeter for Atmospheric CartograpHY) is an imaging spectrometer that was launched onboard ENVISAT satellite by ESA in 2002. Its primary mission objective is to perform global measurements of trace gases in the troposphere and in the stratosphere. The solar radiation transmitted, backscattered and reflected from the atmosphere is recorded at moderate resolution (0.2 nm to 1.5 nm) over the range 240 nm to 1700 nm, and in selected regions between 2000 nm and 2400 nm. The wide wavelength range makes it possible to detect many different atmospheric constituents. SCIAMACHY operates in both nadir and limb as well as Sun occultation viewing mode. It switches between nadir and limb to observe the same air masses from the two directions. The obtained trace gas 'cartography' from the name of SCIAMACHY, however, is limited to the tropopause and higher as limb viewing is only possible for these altitudes, because of the absorption and scattering in the long light path. On the other hand, another advantage is that the ground pixel size for the nadir mode was significantly reduced to 30×60 km^2 (Gottwald, Bovensmann in Lichtenberg, 2006 and de Vries et al., 2007a).
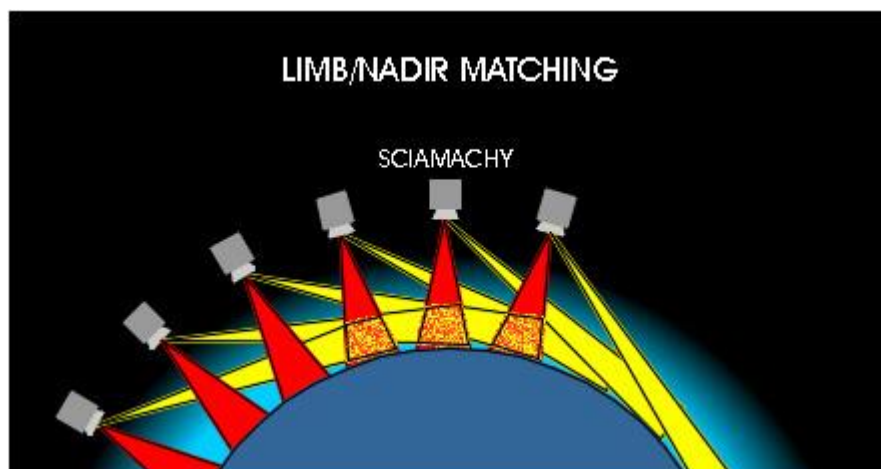
Figure 25: SCIAMACHY viewing geometry. Credit: KNMI

5.3   OMI

Ozone Monitoring Instrument (OMI) is a space-borne spectrometer that was launched in 2004 on board of the NASA's satellite Aura. Aura is part of NASA's long-term Earth Observation System (EOS) mission, which is comprised of a series of coordinated polar orbiting satellites designed to monitor and understand key components of the climate system and their interactions.

The main science objective of OMI is to track global ozone change. Beside the ozone, OMI measures the column amounts of other trace gases (NO_2, HCHO, SO_2, BrO and OClO), maps aerosols and

estimates ultraviolet radiation reaching the Earth's surface. It distinguishes between aerosol types, such as smoke, dust and sulphates. OMI measurements are used to sources and transport of aerosols and trace gases that both affect global air quality and play a role in climate change (Aura, 2011)

OMI is an ultraviolet-visible (270 – 500 nm) nadir-looking imaging spectrograph that measures the solar radiation absorbed and scattered by the Earth's atmosphere. It is a hyper spectral imager with spectral resolution of 0.4 – 0.6 nm. OMI's 2600 km wide swath provides near-global coverage in one day with spatial resolution of 13x24 km^2 at nadir (NASA, 2011).
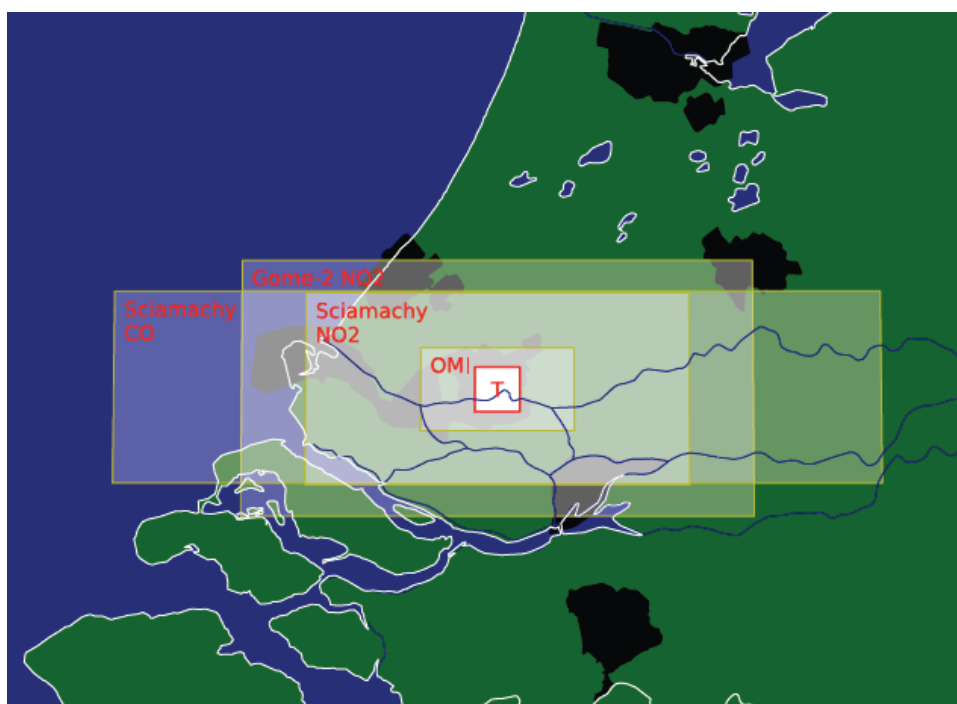
Figure 26: Impression of the 7x7 km^2 footprint of TROPOMI as compared to heritage instruments. The TROPOMI spatial resolution, indicated with the red box, enables to distinguish pollution within large cities. (Stein Zweers et al., 2011).

5.4   TROPOMI

TROPOMI (Tropospheric Ozone-Monitoring Instrument) is a new ESA's mission for troposphere observations. It is the main payload of ESA Sentinel-5 Precursor (S-5P) and is jointly developed by The Netherlands and ESA. Dutch space companies and research institutes participate also in the development of other abovementioned instruments. TROPOMI mission is focusing on global observations of the atmospheric composition for air quality and climate. The planned launch date for S-5P is 2014 with a 7 year design lifetime. Sentinel-5 Precursor will bridge the gap between the end of operation of OMI and SCIAMACHY and technically improved Sentinel 5, expected to be launched in 2020, to provide continuity in global monitoring of atmospheric variables.

TROPOMI will measure the wavelength range from UV-visible (270-500 nm), the near infrared (710-770 nm) and the shortwave infrared (2314-2382 nm). In the UV-visible and near infrared the spectral resolution is 0.5 nm, except for the wavelengths below 300 nm, where the spectral resolution is 1.0 nm; in the shortwave infrared the spectral resolution is 0.25 nm. TROPOMI will have an unprecedented spatial resolution of about 7x7 km^2 at nadir. This higher spatial resolution is very important for the observation of tropospheric trace gases because of the strong spatial gradients occurring for such species (Wagner et al., 2008).
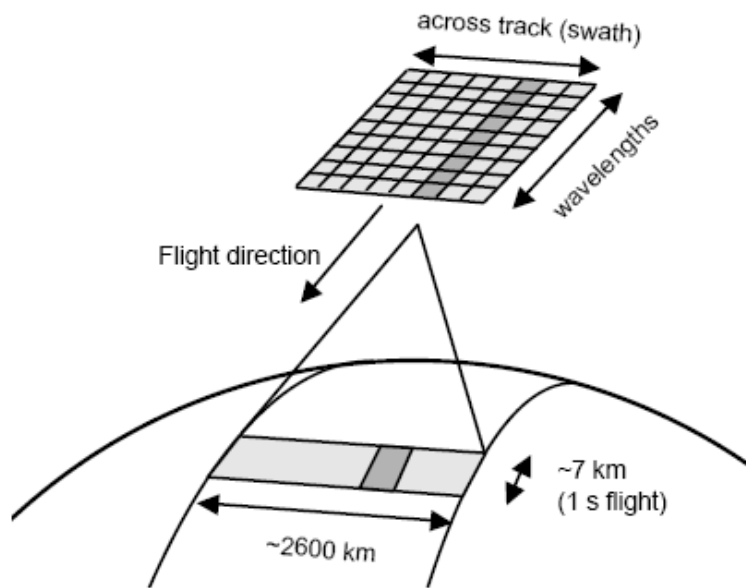
Figure 27: Geometry of TROPOMI observations. (TROPOMI, 2011)

The spatial resolution is combined with a wide swath to allow daily global coverage. The high spatial resolution serves two goals:

- emissions sources can be detected with more accuracy and
- the number of cloud-free ground pixels will increase substantially.

The latter is especially important for TROPOMI data products that are very sensitive for cloud contamination, such as the methane product. In addition to an improved spatial resolution, also the signal-to-noise of TROPOMI will be improved as compared to OMI and SCIAMACHY (Veefkind et al., 2011).
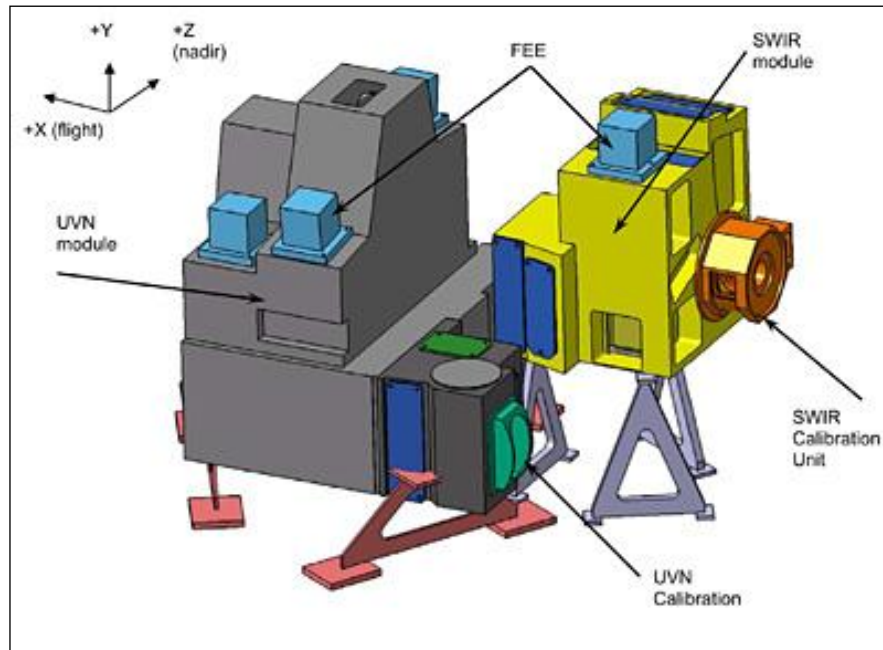
Figure 28: Model of TROPOMI instrument.
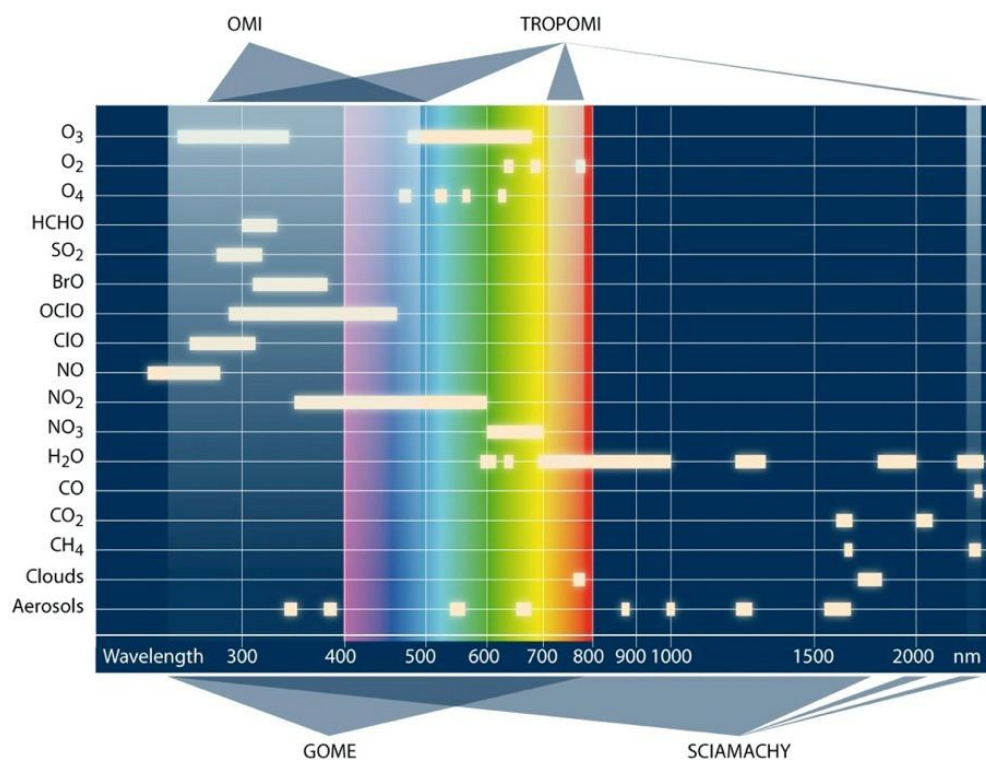
Figure 29: Overview of spectral ranges and trace gas products from SCIAMACHY, GOME, OMI and TROPOMI.

Table 5: Overview of the characteristics of space-borne instruments for trace gas measurements.

Characteristics	GOME	SCIAMACHY	OMI	TROPOMI
Launch date	1995	2002	2004	2014 (plan)
Satellite	ERS-2 (ESA)	ENVISAT (ESA)	Aura (NASA)	Sentinel-5 Precursor (ESA)
Orbit type	Near-polar, Sun-synchronous	Near-polar, Sun-synchronous	Sun-synchronous	Polar
Orbit Height	795 km	800 km	705 km	820 km
Observation Mode	Nadir (whiskbroom)	Nadir (whiskbroom), limb and solar occultation	Nadir (push-broom)	Nadir (push-broom)
Spectral Range	240 – 790 nm	240 – 2400 nm	270 – 500 nm	270 - 2385
Spectral Resolution	0.2 – 0.4 nm	0.2 – 1.5 nm	0.4 – 0.6 nm	≤ 0.25 nm (SWIR) - ≤ 1 nm (UV)
Footprint at Nadir	360 x 40 km^2	Limb vertical 3 x 132 km^2, nadir horizontal 32 x 215 km^2	13x24 km^2	7 x 7 km^2
Swath Width	960 km	1000 km (max)	2600 km	2600 km
Global coverage	3 days	6 days (repeat period 35 days)	1 day	1 day

TROPOMI instrument is technically significantly improved and is better than other instruments in all categories. The most important improvement is better spatial resolution – it is six times higher as OMI's (7x7 km^2 vs. 13x24 km^2) and more than hundred times better as SCIAMACHY's (32x215 km^2). Despite good spatial resolution, enough energy is captured to provide one to five times higher signal-to-noise even for very low albedo. High SNR guaranties higher reliability of measured features. GOME's and OMI's prior mission is to observe ozone layer in stratosphere. With observations in short wave infra red (SWIR) part of the spectrum, SCIAMACHY broke the ice in space-borne detection of greenhouse gases such as CO and CH_4. TROPOMI is, on the other hand more focused on chemical conditions of the troposphere. To attain enough information on the layer, which is often hidden under

the clouds, TROPOMI makes use of better algorithms for assessing the impact of those particles on light propagation. Smaller pixel size makes it possible not only to observe the distribution of atmospheric chemicals but also to detect their origins and to connect their pattern with certain issue (traffic, biomass burning, volcanic eruption...).

A new generation of UV/VIS/SWIR satellite instruments has allowed one to measure backscattered solar radiance from the Earth over a large wavelength range. From the measured spectra several important tropospheric trace gases (e.g. O_3, NO_2, NO_3, $OClO$, SO_2, BrO, H_2O) as well as clouds and aerosols can be determined from space. SCIAMACHY and TROPOMI with their additional spectral channel in SWIR also allow the retrieval of greenhouse gases (CO_2, CH_4) and CO. A wide range of important issues is studied based on the data provided by above mentioned instruments (KNMI, 30.8.2011):

- ➢ the trend in the ozone hole and a possible recovery of the ozone layer in the future,
- ➢ the amount and global distribution of air pollution,
- ➢ changes in the amount of human-related emissions (such as fossil fuel and biomass burning) and natural emissions (*e.g.* emissions from soils and vegetation, lightning),
- ➢ trends in ozone in the lower atmosphere related to these changes in the atmospheric composition,
- ➢ the relation between changes in ozone and the greenhouse effect,
- ➢ derived global distribution can serve as input and for the validation of atmospheric models,
- ➢ etc.

6   TIDE – TROPOMI INTEGRATED DEVELOPMENT ENVIRONMENT

6.1   Presentation of the software

TIDE is a grid based software simulation tool, which was developed by Dutch Space in the framework of design studies for TROPOMI instrument. It simulates TROPOMI Level 2 products retrieval and their errors and is used to evaluate instrument's performance.

There are three levels of data products gained by space-borne spectroscope. Level 0 data is the measured signal detected by CCD detector. Level 1b data products comprise geolocated and calibrated radiances of the scientific measurements. Level 2 data are column densities and profiles of atmospheric constituents.

There are several partners cooperating in the TROPOMI project, each taking care of its own share of the instrument development. However, technology is not capable to fulfil all scientists' ideas and expectations and trade-offs where technological complexity and cost must be traded with instrument performance as well as with the effects on the value for the user must be done. TIDE was created to make the process of making trade-offs much more efficient and less time consuming. It gathers simulation elements of different partners and makes them reachable for everyone of them. If one party decides to change some design parameters it can immediately check the effect of this change on the whole chain of retrieval process. Thereby TIDE makes it possible to optimize the instrument hardware requirements during the development cycle.

The main elements in the TIDE computing chain are:

- Scene generator,
- Exposure generator,
- Radiative transfer models for UV-NIR and SWIR,
- Instrument simulator,
- Level 0-1b processor,
- UV-NIR/SWIR level 2 retrieval, and
- Error combiner.

As written in TIDE documentation (de Vries, 2010), the chain is executed in a grid environment to firstly make use of its natural parallelization, as the scene generator is applied once per simulation, the instrument simulator, level 01b processor and product algorithms are used once per swath and the radiative transfer models once per scene pixel. Secondly, the Dutch Space GridAssist toolset is used that takes care of all workflow and access handling management and provides the distributed environment to allow all partners to access the TIDE. It also allows providing the modules as

executable tasks thereby safeguarding the proprietary aspects of the software for all partners separately.

TIDE is accessible via internet from the TROPOMI/TIDE portal on the web page http://grid.dutchspace.nl/tropomi/index.html. The portal is used to start the GridAssist workflow tool, the tool to control TIDE runs. A valid username and password are needed to login. Once the tool is started it is automatically downloaded so it is possible to have a direct link to GridAssist from our desktop and thereby bypassing the portal for other runs. To run the tool Java Runtime Environment needs to be installed on the computer.

6.2   Grid computing system hidden behind TIDE

TIDE makes use of the GridAssist software framework, which in turn utilizes a grid computing system. GridAssist is therefore the grid tool and TIDE is GridAssist with the set of executable task available. Grid computing is a form of distributed computing where a virtual computer is created, consisting of a cluster of networked computers that act together to perform large computing task. GridAssist provides the benefits of computing in a grid environment to applications that are not inherently 'grid-aware', for users who are not experts on grid technology. It provides a portal for access to applications, resources and data using high-speed networks, a scenario builder and a controller for scheduling jobs (de Vries, 2010).

6.3   Building a workflow

A key component of GridAssist is its graphical user interface. Behind the GUI is hidden a lot of complex technology that the user do not need to be aware of. An example of the GUI created by GridAssist is shown in Figure 30.
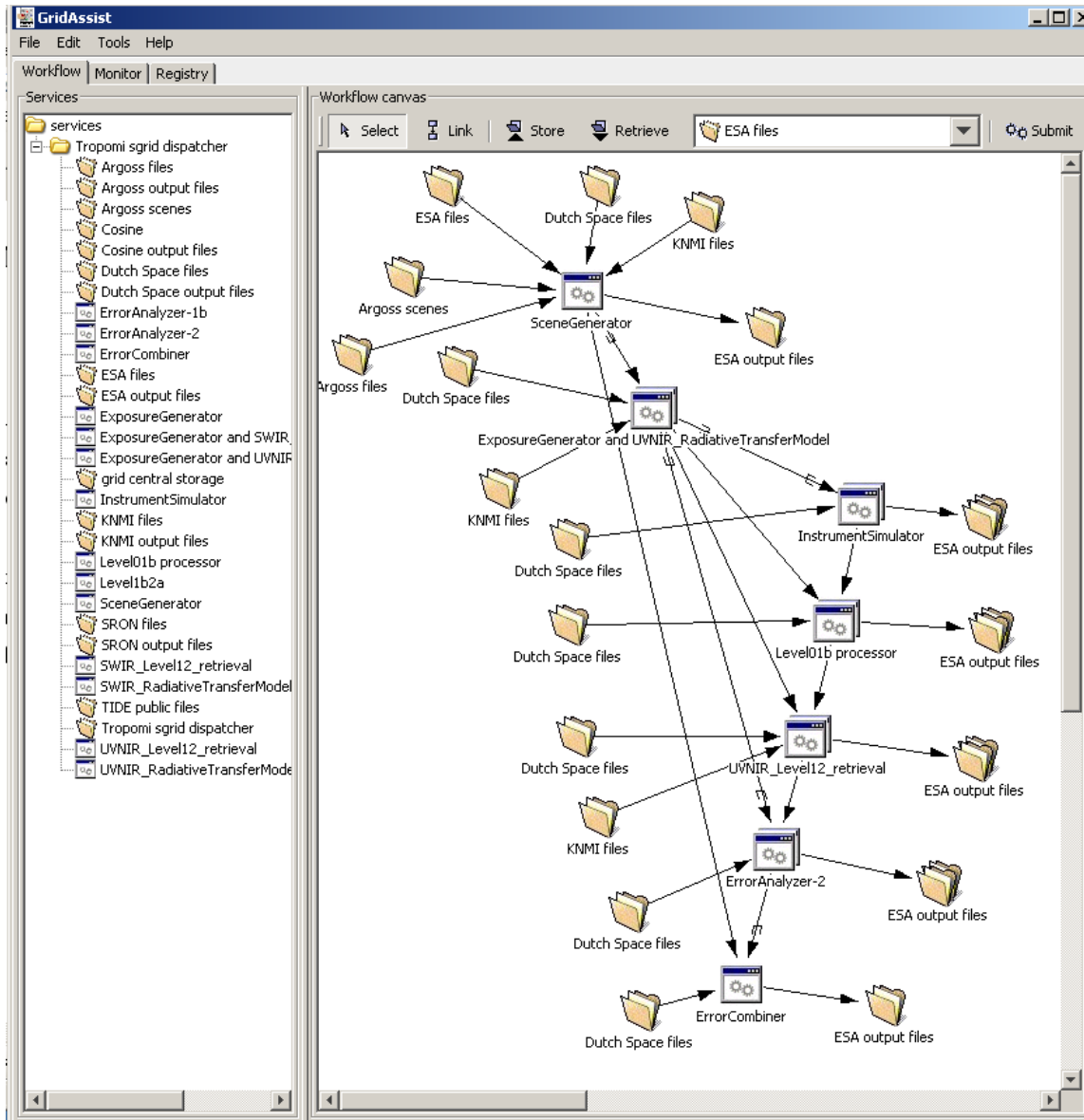
Figure 30: GridAssist workflow for TROPOMI

On the left-hand side of the window is a list of data storage directories and executable programs – applications, which can be used in the simulations. The workflow canvas on the right-hand side is originally empty and is meant to create desired workflows in it. The user can construct workflows using drag-and-drop principle – the user drags the needed files from the list on the left and drops them on the right panel. Between applications themselves and between application and data storage, data connections need to be established. Each application demands certain input data. For each connection the user has to define which data should be transferred. Very helpful here is the list of for the application needed data with expected name and format that opens always when the connections are being set. The user than has to connect the corresponding file to each suggestion in the list. The files

that are transferred can be viewed by moving the mouse over the connection. The workflow tool checks the correctness of the connection between the services.

After submitting the prepared run the progress of the job can be tracked in the Monitor tab. There the job can also be stopped and/or deleted.

6.4   Processing flow

The basic processing flow in TIDE is presented in the Figure 31.
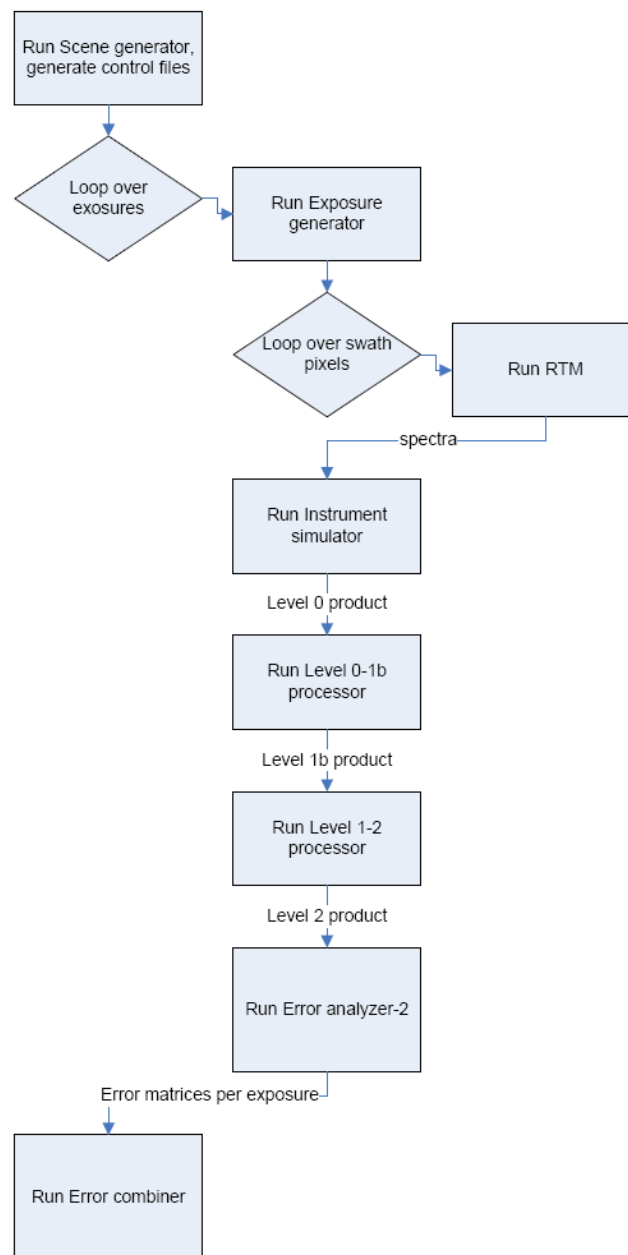
Figure 31: Basic processing flow in TIDE (de Vries, 2010)

Scene Generator generates a (test) atmosphere/orbit in a form of a series of inputs to the *Exposure Generator*, which is an extension of the Scene Generator, meant to help double-loop parallelism for the Grid system. The next module is *UVNIR/SWIR Radiative Transfer Model (RTM)*. This module generates radiance spectra from the input scene created by scene generator considering the information from Exposure Generator.

Instrument Simulator takes the radiance spectra and produces raw measurement data, taking into account the instrument optics and detector and electronics performance in terms of noise and systematic errors.

Level 0 to 1b Processor converts the raw measured signal created by Instrument Simulator into calibrated radiances, while the *UVNIR/SWIR Level 2 Retrieval* contains the level 1b to 2 retrieval algorithms for NO_2 or CH_4 and CO. The goal of the level 1b-2 data processing is to provide geophysical parameters as column densities and profiles from atmospheric constituents as well as cloud and aerosol parameters. At the end of the whole chain there are *Error Analyser* that compares the initial (test) atmosphere with the retrieved (level 2) products and the *Error Combiner* a simple module that combine the outputs from Error Analyzer as it is processing single exposures only. (de Vries, 2010)

Scene generator reads the input data – meteorological data, trace gases, albedo, surface elevation and clouds. Meteorological data consists of the following parameters: H_2O (ppmv), pressure (hPa), surface pressure (hPa), and temperature (K), and is given for each pixel of the scene in 20 vertical layers (surface pressure only in one). Trace gases (NO_2, O_3, SO_2, CH_4 and CO) distribution is given in 12 vertical layers – for the troposphere only. Combined UV and visible channel, named UVIS channel (310 – 496 nm), which was used in our simulations does not need the surface elevation model; however, it will be needed in SWIR channel. Albedo is also given 11 layers, yet here the layers are not according to the altitude (surface albedo correspond only to the surface) but to different wavelength.

The reading of scene describing data scene generator defines the orbit according to selected starting latitude and longitude of observation. Satellite (Sentinel 5 Precursor) will orbit the Earth in LEO Sun synchronous polar orbit at an altitude of 820 km. On Figure 32 the default orbit used in the tool is shown.
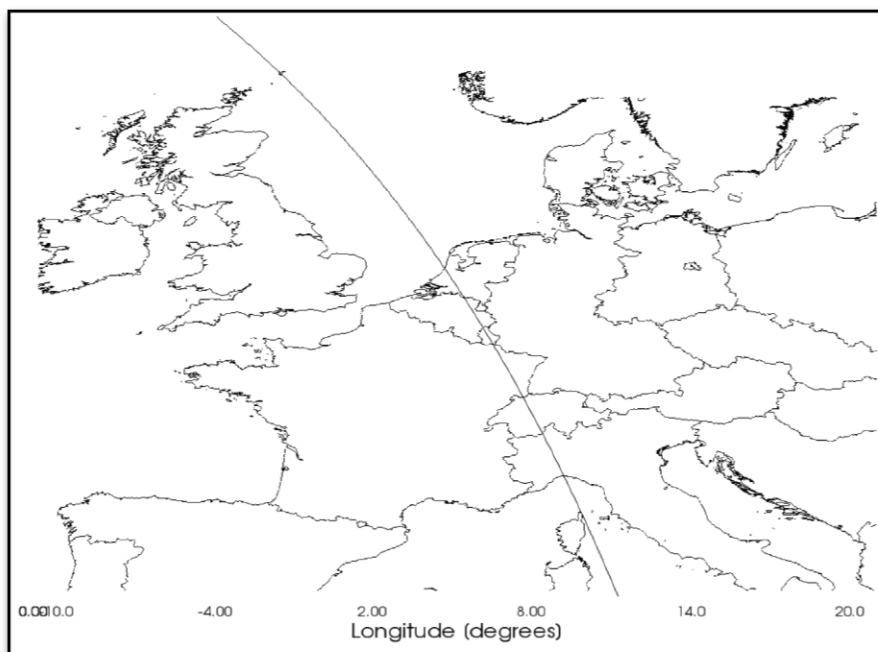
Figure 32: Default orbit (de Vries, 2010)

The orbit is needed to generate the observational grid. The exposures are taken in nadir mode with instrument swath field of view is 108°. The observational grid is not aligned with the scene data and covers wider area as the area with the predefined scene. Therefore, it is possible to limit the grid from the orbit to the scene. This setting avoids computation of exposures and swaths outside the scene, apart from residual corners due to the fact that the observational grid is rotated as compared to the input scene. Because of the rotation, the input scene must be re-gridded. Each of the scene pixels is divided in (by default 8 x 8) smaller pixels. The scene is covered by the observational grid. The smaller scene pixels that have their centre inside the same observational grid pixel are then averaged and the average is written to corresponding pixel of the observational grid. Re-gridding is performed for all scene elements, separately for every layer. After the re-gridding of the scene the radiative transfer model (RTM) can be performed to calculate the radiance for each pixel (de Vries et al., 2007).

Instrument simulator simulates the performance of the instrument. All the main characteristics of its design, the optics, grating, detector and electronics are taken into consideration. This module takes the radiances as in input and gives as an output digital numbers that correspond to the detected signal for each wavelength, i.e. level 0 data. Level 0 to 1b processor converts the digital numbers into the number of photons that hit the pixels – level 1b data. Level 2 data are trace gas total columns in molecules per square centimetre.

7   ANALYSES AND RESULTS

In the framework of this research I was trying to estimate the accuracy of the retrieval of gas profiles and its sensitivity to the error sources, in particular to detector noise, stray light and spectral mis-registration within the spectrograph. This job has been done in the framework of TROPOMI instrument design. My job was to test TIDE: if this tool is good enough and at the same time sufficiently simple to be used in final simulations of the instrument. Simulations of the instrument performance, which are needed in the design process to check how the overall performance changes if some design parameter is modified, have been done. On this topic an article has been written which I presented at the EARSeL 7th SIG-Imaging Spectroscopy Workshop in Edinburgh in April 2011 and was published in the conference proceedings (Urbas, Esposito, de Vries, 2011).

TIDE simulates a hyper spectral imaging spectrograph. As such it demands an enormous amount of different input data. Input files are originating from six different research groups: Agros, Cosine, Dutch Space, ESA, KNMI (Koninklijk Nederlands Meteorologisch Instituut – The Royal Dutch Meteorological Institute), and SRON (Netherlands Institute for Space Research). Although I got the workflow already set with all necessary connections between input files and applications, study of these files was needed before starting using the software. Some data can be reviewed by the user, the others (like retrieval algorithms) are at disposal for usage but have the code hidden. After getting familiar with the data flow I set the parameters for desired analysis (testing the effect of instrumental noise, stray light within spectrograph and spectral mis-registration). Analyses are described in this chapter.

The analyses demonstrated that TIDE has the potential to be used to simulate the instrument to finalize its design but it needs to be upgraded. Right now it is still incomplete and does not give reliable answers.

This chapter gives the description of the work that has been done, the obtained results and their comment. All simulations were done with TIDE.

7.1   General settings

First general settings were selected. These include the observed area, scene parameters, orbit, wavelength channel, and trace gas to be retrieved and requires at least basic understanding of how TROPOMI works. Scene is described with meteorological parameters (temperature, pressure, water vapour, cloud fraction), concentration of different trace gases (NO_2, O_3, SO_2, CO, CH_4), orbital parameters and wavelength- and monthly dependent surface albedo. Scene parameters are given in several vertical layers.

The choices for general settings were limited with the existing data that could be used. The simulations can be done for any part of the globe but the scene parameters are for now prepared only for the area of the Netherlands in better resolution or for (part of) Europe in worse resolution. Slovenia is on the very edge of the Europe scene, not entirely covered; therefore the area of the Netherlands was selected. The scene parameters were prepared for above mentioned areas for every hour of August 2003 and January 2007 considering all existing data for this area and period. For the analyses, the scene conditions of January 5, 2007 at 13:00 were selected on basis of images of clouds and trace gases distribution (Figure 33) – partly polluted with NO_2 and with quite some clouds with clear air in between.
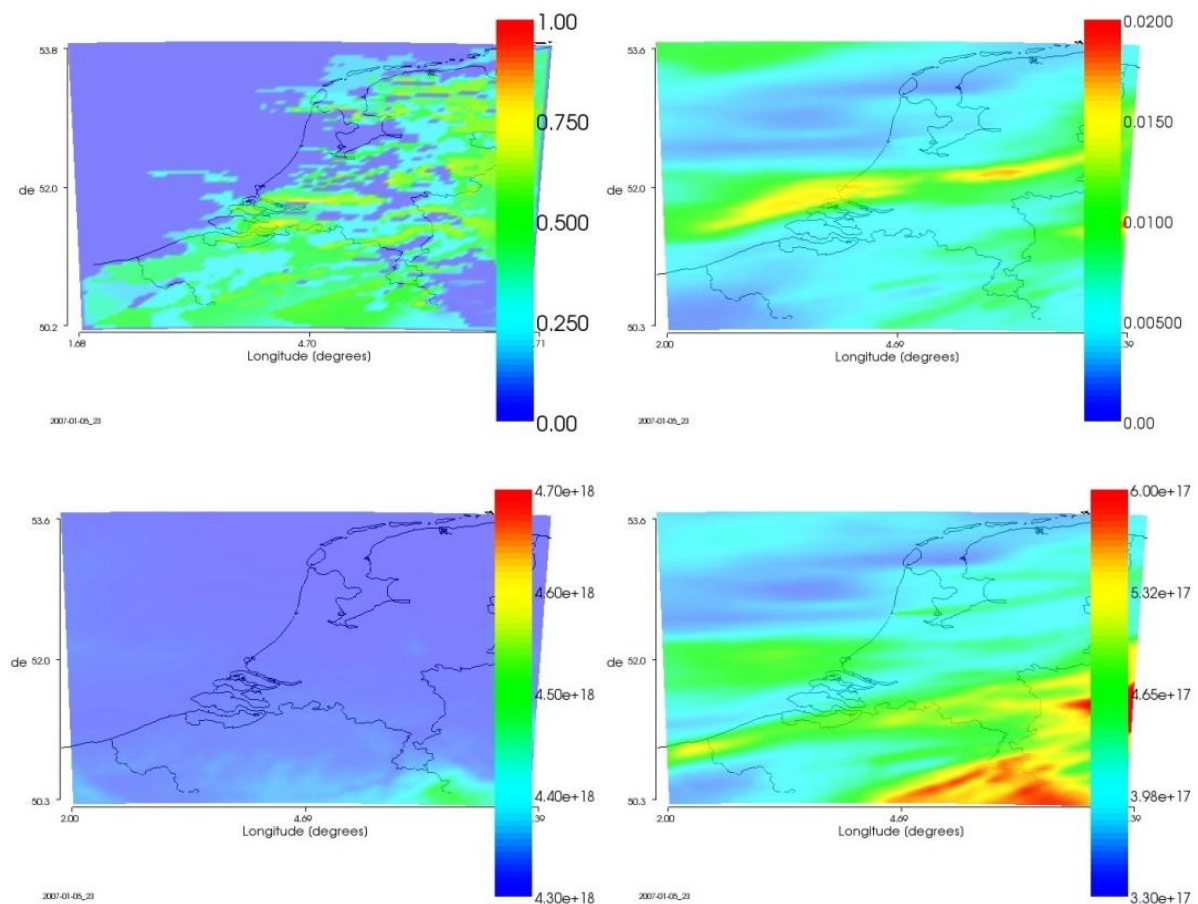
Figure 33: The selected scene used in the simulations. Images in the upper row present the cloud fraction (left) and NO_2 concentration (right), in the bottom row there are CH_4 (left) and CO (right) distribution. On the image also the observed area of the Netherlands can be seen.

From the images of the scene also the geographical area under consideration can be seen. The observational grid from the near polar orbit is not aligned with the north-oriented observed area but it is limited to the scene – includes all and only those exposures that contain at least one scene pixel and

each exposure is cut to form the smallest rectangle around the scene. Therefore, there are empty corners with no scene in the observational window (Figure 34).

The next restriction was on the choice of the wavelength channel. Currently only the UVIS channel can be used. System design is being upgraded for the SWIR channel and is currently being tested. For UVIS channel the level 1b to 2 retrieval algorithms are available only for NO_2. A newly implemented slant column algorithm allows also the retrieval of the other UVN trace gases, but this is also in the test phase.

Other basic settings were as follows:

- instrument design settings: BOL (beginning of life, like it will be just after launch)
- observational window: 79 exposures, 71 pixels (matrix with 79 rows and 71 columns)
- coordinates of observational window:

(φ, λ)	W	E
N	53.17°, -0.38°	54.93°, 7.01°
S	48.93°, 2.59°	50.53°, 9.40°

- part of the swath: nadir, extreme viewing zenith angles are -18° and +17°
- wavelength channel used: UVIS (310 – 496 nm)
- trace gas being retrieved: NO_2

7.2 Simulations done

A matter of interest were the effect of noise in the system, the effect of different stray light fractions introduced in the level 0 to 1b processor on the retrieved total column of NO_2, and the effect of spectral mis-registration. The questions that we wanted to answer are:

- What happens if the stray light turns normal limits?
- How does the presence or absence of the clouds result in stray light effect on the retrieved parameters?
- What is the effect of spectral mis-registration?
- In addition, we checked how the instrument performance is about to change during the lifetime of the instrument.

According to the desired analysis the series of needed simulations was specified:

➢ reference run with no instrumental error included in the run,

➢ run with noise effectuated in the level 0 product – to estimate the effect of noise,

➢ run with stray light fraction 0.036 introduced to the inverse model (stray light fraction in forward model is set to 0.018) – to estimate the effect of stray light,

➢ run with noise for EOL,

➢ series of runs with different stray light fractions, and

➢ series of runs with different mis-registration error

7.3   Reference run – results

Reference run was executed with the general settings described above but with all possible error sources originating from the instrument design excluded. It was obtained simulating a perfect instrument. The result (see Figure 35) was free of noise and stray light effect, i.e. free of instrument errors.
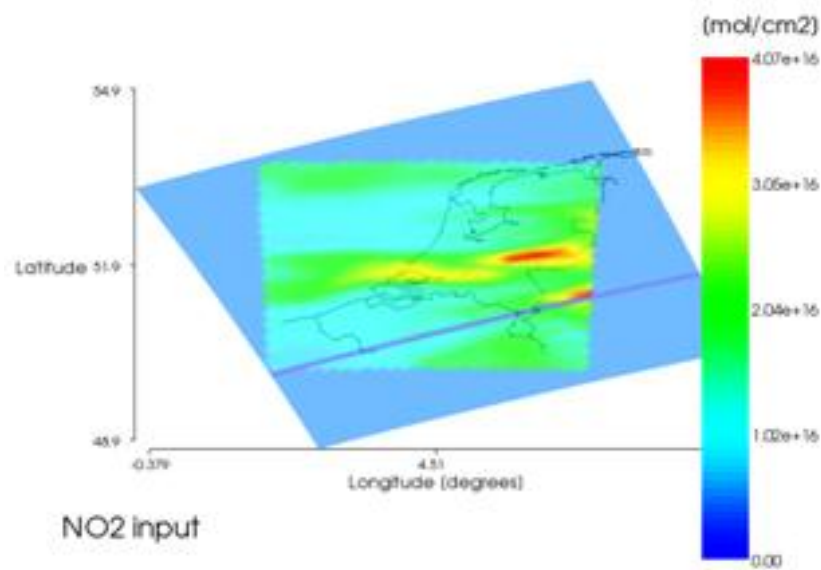
Figure 34: NO$_2$ as an input data in the trace gas retrieval simulations
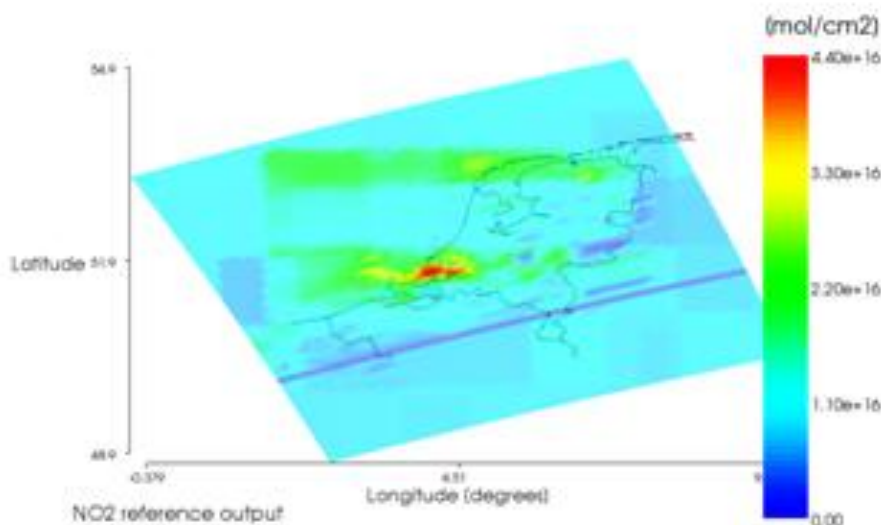
Figure 35: NO₂ result of the reference run simulating a perfect instrument

The images on Figure 34 and Figure 35 are considerably different, although there was no instrumental error in the reference run. The deviation is due to the incomplete air mass correction in the retrieval algorithm, which presently does not include the iterations to accurately retrieve the vertical trace gas profile. Therefore, as the name implies, the result (retrieved NO_2 total column) of the reference run was used as a reference in all further analyses instead of the NO_2 vertical columns that were used as an input. Very noticeable is also the chessboard pattern, an impact of surface albedo, which is given in 1°x1° resolution.

The relative error was calculated using equation (19) to estimate the accuracy of the whole system:

$$NO2_{error} = \frac{NO2_{input} - NO2_{result}}{NO2_{input}} \tag{19}.$$

For all scene data containing pixels in the observational window the root mean square (RMS) was calculated. Its value of almost 46% support the conclusion obtained from visual comparison of the above images, that the deviation is relatively large. Another detail that cannot be overlooked on Figure 34 and Figure 35 is a missing line. The reason for this is that DAK, the radiative transfer model used for UVIS channel, obviously failed in one exposure so the radiances there were not calculated. This was not supposed to happen and the cause was not found yet. Nevertheless, other exposures were calculated properly, therefore the missing line was overseen in the analyses and excluded from calculations.

7.4   The effect of noise on the retrieved NO_2 total column

Noise refers to random, non-deterministic errors that vary over time relatively quickly in relation to an orbital period. in a way that cannot be predicted or estimated, in which there is no correlation between successive realisations, so that it cannot be decomposed in a simple series of elementary harmonic errors (S5p SRD, 2011). Total column is a slant path that the light travels from the Sun to the satellite after reflecting from the Earth.

Important measure in science and engineering is signal-to-noise ratio (SNR). SNR compares the level of a desired signal to the level of background noise and is defined as the ratio of signal power to the noise power. TROPOMI tends to detect also some trace gases with very low concentration, therefore considerably high SNR with values between 100 and 1000 (depends on the channel) is necessary. To achieve high SNR, signal has to be strong and noise as little as possible.

To estimate the effect that noise in the spectrometer has on the retrieved NO_2 total columns the run with noise effectuated in the level 0 product (measured signal) was prepared. Adding noise in the simulation means that all pixel signals are replaced by a random variation based on the total variance associated to the pixel. Random distribution of the noise can be seen on NO_2 result of the 'noisy' run (Figure 36). RMS of the NO_2 errors is 0.49, which means that the retrieved total columns are on average almost 49 % different from the true value.
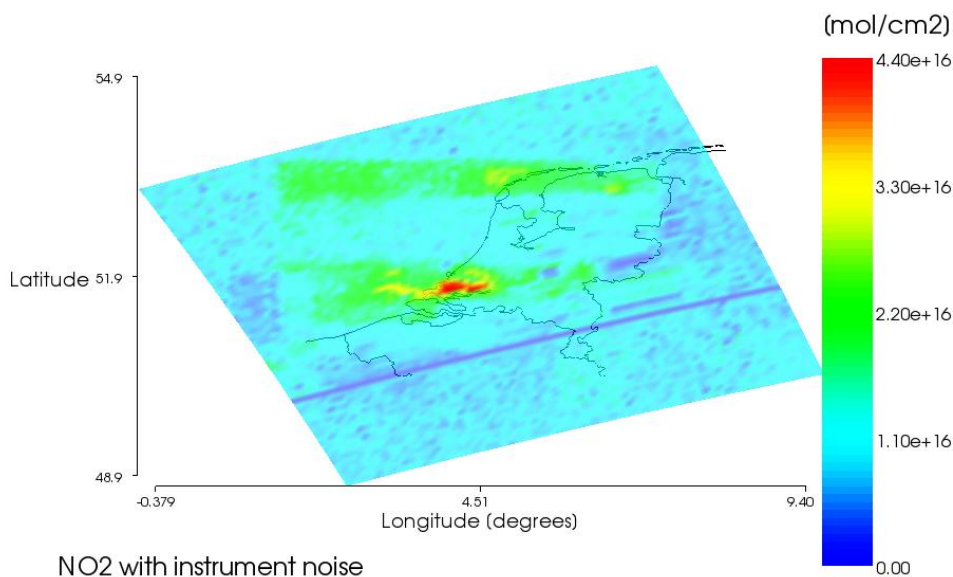
Figure 36: NO_2 total columns obtained from the 'noisy' run

The noisy results were compared to those of the reference run. Following the structure of equation (19) the relative effect of noise on the retrieved total column of NO_2 was acquired. From the result (see

Figure 37) we can see that the noise is randomly distributed (following Poisson distribution, approximated as a Gaussian – normal) all over the observational grid and that there is no viewing zenith angle dependence.
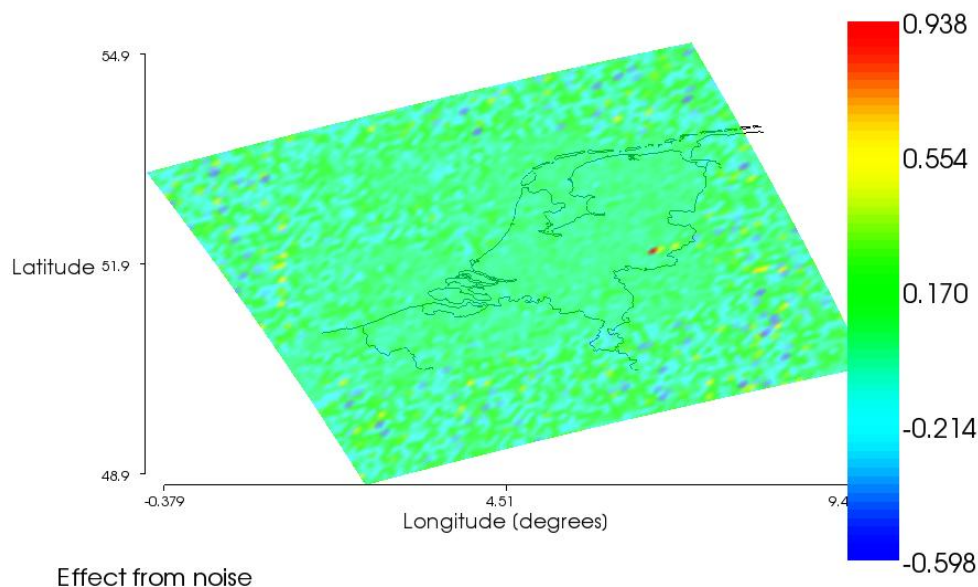
Figure 37: Spatial distribution of noise effect

The above results are all obtained for the instrument parameters as they will be at the beginning of life (BOL) of the instrument. To assess the effect of aging of the instrument on the spectrograph's noise, additional run with noise using the EOL instrument design file has been done. EOL conditions are estimated according to examples of the previous instruments (OMI, GOME). Compared to BOL, EOL have seven times bigger detectors dark current and the optics throughput decreased by 10%. Noise distribution was the same as for BOL, therefore also the shape of the histogram was almost the same. Because of slightly bigger noise values in all pixels, the histogram is a bit more spread out but equally shaped. All calculated RMS are for about 1% larger for the end of life as they are supposed to be after the launch.

Calculated RMS values are as follows:

Table 6: The effect of noise on the NO_2 retrieval

	BOL	EOL
RMS of the NO_2 error of reference run	45.78 %	45.78 %
RMS of the NO_2 error of run with noise	48.56 %	48.93 %
RMS of the noise effect in NO_2 retrieval	11.11 %	12.08 %
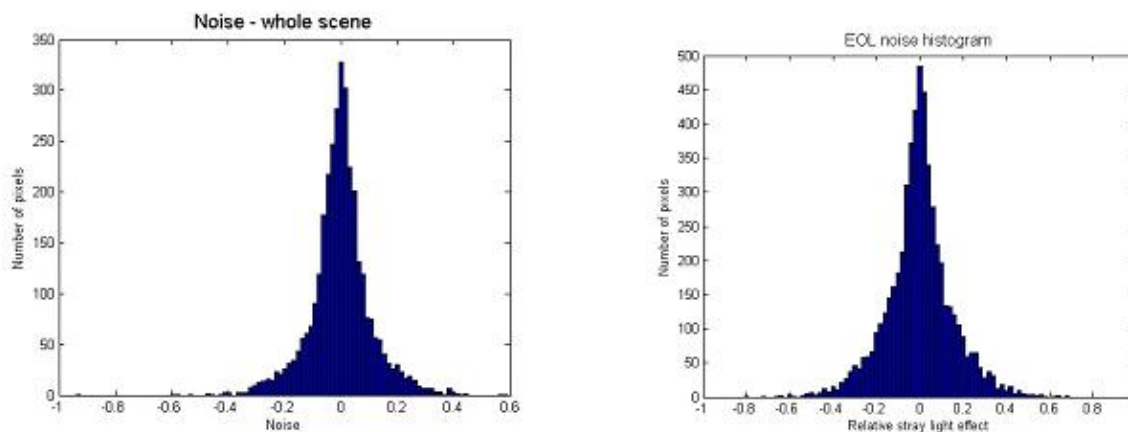
Figure 38: Noise histogram for BOL (left) and EOL (right) instrument design

7.5   The effect of stray light on the retrieved NO$_2$ total column

Similar to the noise analyses, the effect of stray light in the system has been analysed. Like in the case of noise the results were compared to the reference run simulating perfect instrument. Stray light is external light from any spatial or spectral dimension being recorded on a detector pixel where it is not intended to be recorded (S5p SRD, 2011). In the analyses stray light refers to uniform stray light, which is dependent on detected signal but not on wavelength and viewing angle. Ghosts are expected to be negligible.

Several runs have been done with different stray light fraction induced to the level 0 to 1b processor. First, all runs were done with BOL instrument design file. Stray light fraction used in the forward model remained the same for all simulations, 1.8 %. In the inverse model half (0.9%), double (3.6%) and four times bigger (7.2%) stray light fraction was used as compared to the one in the forward model. The effect of wrong calibration of stray light is presented in Table 7. As stray light depends on clouds on the optical path of the light, in the Table 8 results are given in dependence to the cloud density.

Table 7: Effect of different stray light values on NO$_2$ total column

[%]	SL 0.9	SL 1.8	SL 3.6	SL 7.2
SL effect	0.1	0.0	0.6	1.6

Having the same stray light fraction in both models yields total elimination of the stray light effect. On the other hand, bringing different stray light fraction in inverse model than it is in forward model

means introducing an error in the stray light calibration. When inverse is close to forward stray light the calibration error is small - well below 1%, but it grows to 1.6% if the stray light is estimated wrongly for factor 4. Therefore, one can conclude that the contribution of wrong estimation of stray light in its calibration algorithm to the error budget is relatively small in comparison to the contribution of noise.
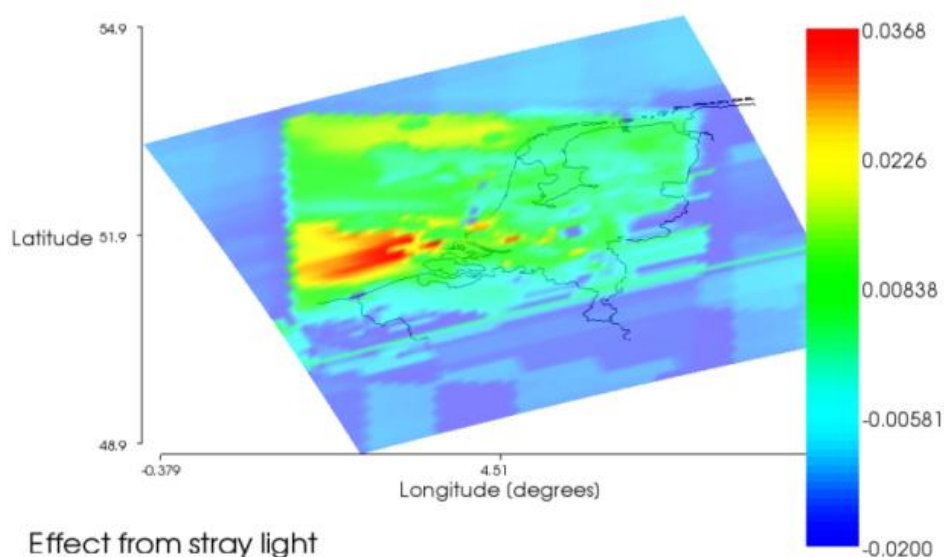
Figure 39: Effect of stray light on NO$_2$ retrieval

Comparing the image of stray light effect (Figure 39) and the cloud distribution (Figure 33) we can see that the stray light effect is smaller for cloudy areas than for the areas without clouds. Cloudy areas are regions with high effective albedo/radiance level.

Table 8: Relative effect of noise and/or stray light on NO$_2$ result in dependence on cloud density

	No clouds	Little clouds (0-0.33)	Dense clouds (0.33-0.66)	Heavy clouds (>0.66)	All over the scene
Noise BOL [%]	11.91	10.18	11.88	11.84	11.11
Noise EOL [%]	13.02	11.03	12.91	12.79	12.08
SL 0.9% [%]	0.09	0.08	0.10	0.23	0.10
SL 3.6% [%]	0.62	0.48	0.68	1.69	0.64
SL 7.2% [%]	1.57	1.19	1.67	4.13	1.61
Noise (BOL) + SL 3.6% [%]	12.64	10.50	12.40	12.87	11.63
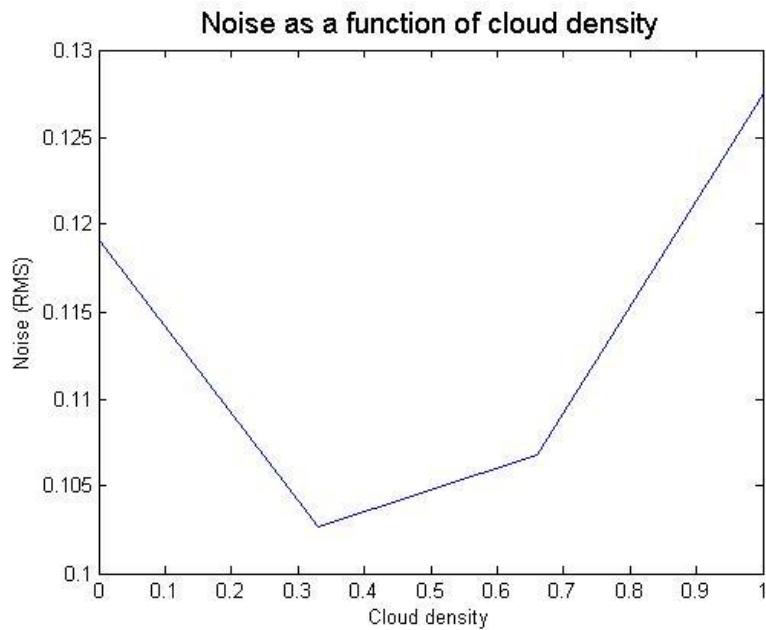
Figure 40: Graph of the BOL noise as a function of cloud density

7.6   The effect of spectral mis-registration on the retrieved NO$_2$ total column

To evaluate the effect of spectral mis-registration five test error cases on wavelength knowledge have been performed. In each test case a different error (10 pm, 50 pm, 100 pm, 300 pm, 500 pm) was injected in the level 0-1b processor.
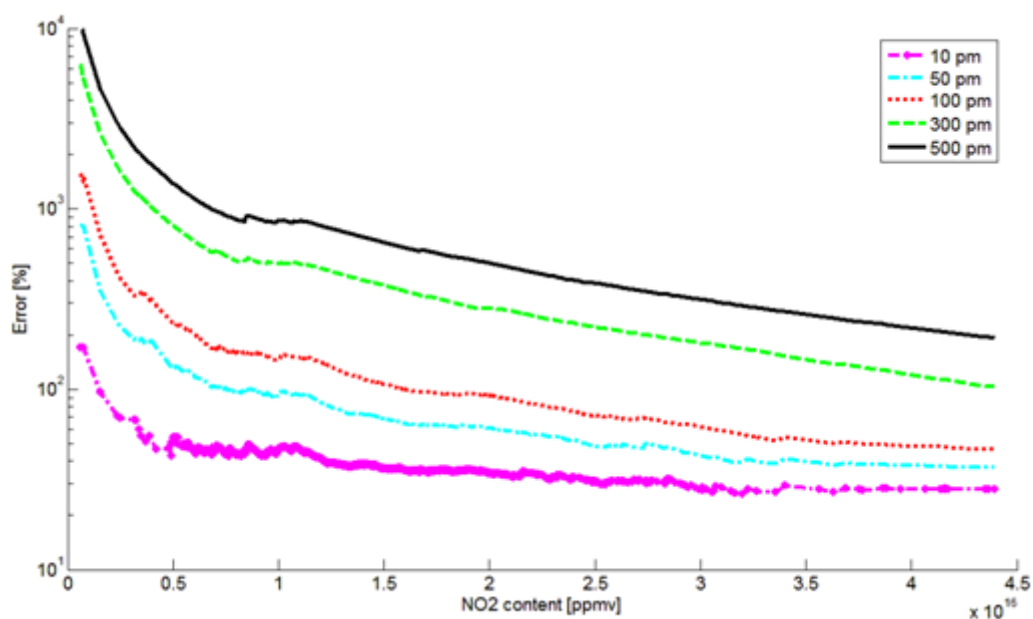
Figure 41: NO$_2$ error caused by mis-registration as a function of NO$_2$ content

The error on the NO$_2$ retrieval as a result of spectral mis-registration is large. A mis-registration of 10 pm on the wavelength knowledge induces an error of about 50% for the NO$_2$ density level most present in the selected scene (between 1 and 2 x 10^6 ppmv as shown in Figure 42). With the NO$_2$ content the error decreases and stabilizes around 28% for high NO$_2$ content. The 10% accuracy requirement is therefore already exceeded for a mis-registration of 10 pm. Even though in orbit wavelength calibration is possible, and therefore the wavelength knowledge can be recovered once these errors occur, further simulations with smaller mis-registration errors need to be performed.
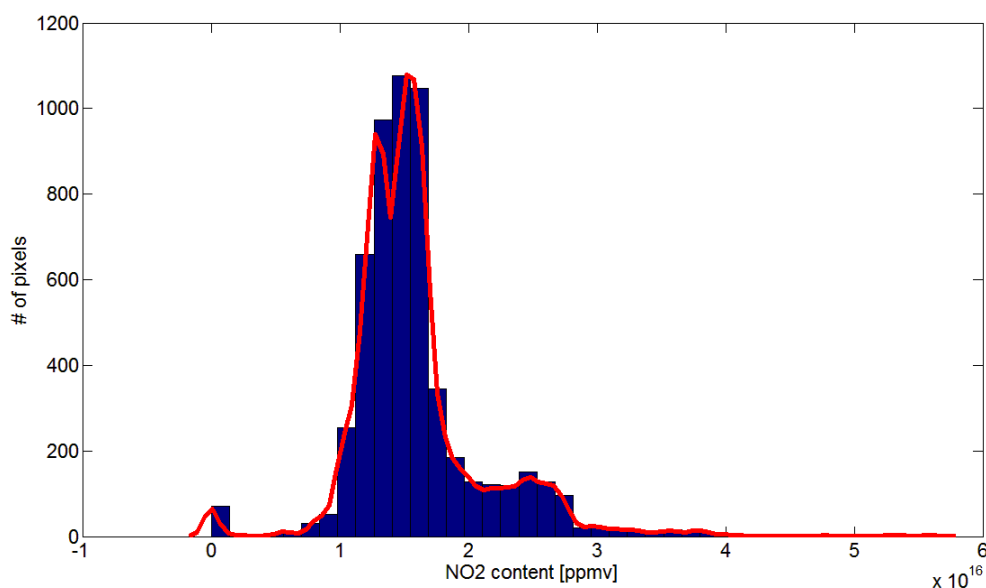
Figure 42: Histogram and graph of NO$_2$ content distribution over the scene

Summarising the results of performed analyses, we can see that the contribution of noise to the total instrumental error budget is much bigger as it is of stray light. Noise causes the error of around 10%. This error becomes slightly bigger after years in orbit. Stray light effect is for factor 10 smaller – error is below 1%. Stray light is largely eliminated by calibration. For tested values mis-registration causes huge errors (50%). From these results the importance of accurate spectral calibration is obvious.

The instrument requirement is that instrumental errors should not affect the retrieved gas total column for more than 10%. The results do not fulfil this requirement. There are two possible outcomes: or the simulation is not done properly or the instrument design is not good enough. As TIDE is not yet complete and is still being upgraded, it is most likely to be responsible for the deviations. After all, TROPOMI is designed following the heritage of experiences of its very successful predecessors.

7.7   Discussion

Running the simulations with TIDE is not a very straightforward task. It requires at least basic theoretical background and understanding of how the simulation tool is set. For a new user it takes some time to get familiar with it. For me, kind explanations given by the author of the tool, Mr. Johan de Vries, were indeed very helpful. Nevertheless, during my work with TIDE I have come across some problems.

The first simulations gave completely unreasonable results – the NO$_2$ error was estimated to few million percents. After excluding all possibilities that the error was done by the user while setting the

settings, the bug was found in the code to which the user cannot access. The problem was that the radiances were not calculated over the scene but on the very edge of the swaths where there was no scene data. The scene was in the middle of the swaths. Therefore, comparing those results to the data that was supposed to be the input gave such a big retrieval error.

Another difficulty represents the missing line in the retrieved data. The reason for this is in the radiative transfer model that calculates the radiance, which failed for one exposure. Why this happened has not been detected yet.

Simulation of a hyper spectral imager is a computationally very demanding task. There is an enormous amount of mathematical operations behind the simple GUI of the simulation tool and because of this the simulations are very time consuming. it took more than 24 hours to get the results of the simulation of instrument performance above the selected area of the Netherlands. Running the same task on one computer only instead of using the grid computing system would take weeks. Because of the considerable amount of output data the downloading of it from shared folder of the program to personal computer also lasts a couple of hours; so the program cannot be used meanwhile. Furthermore, running more than one task (defined by the same or different users) at the same time makes the program run even slower and is therefore not recommended.

The analyses were used not only to estimate the effect of different design parameter on the TROPOMI instrument performance but also to evaluate TIDE as a simulation tool. After a series of unreasonable results a bug was found in the system and the inconsistencies were corrected. Therefore I can say that my research for the thesis contribute its share also to the real project, to the upgrade of TIDE.

8   CONCLUSIONS

Observing the atmosphere, the gas layer that makes the life on Earth possible, is observing the invisible for the human eye. When we look at the sky there is, apart from blue sky and the clouds, not much that can be observed in the real sense of the word. But there is a lot that can be measured with modern instruments. Imaging spectrographs can provide reliable information on different gases and particles in the atmosphere. Changes in its composition can and already do affect animal and plant species and are even more fatal to more sensitive species. With regular observations it is possible to control emission sources and sinks. And to take actions until the atmosphere can recover. Satellite observations of trace gas distribution provide information in support of European and World policies. Services include also monitoring of air quality.

The actuality of the climate related issues was one of decisive arguments for me to choose this topic for my diploma thesis. During my research I became familiar with a very powerful and promising technique for obtaining necessary data and information. Spectral imaging has great attribute that enables simultaneous detection of several different atmospheric constituents at wide wavelength range with the same instrument. It is also suitable for space-borne observations that provide global coverage in high temporal and moderate spatial resolution, which are the same for every part of the globe.

Practical part of this thesis was done during my stage at European Space Research and Technology Centre (ESTEC) in Noordwijk, the Netherlands, where I got a unique opportunity to cooperate in the process of developing a new satellite instrument TROPOMI. I was using TIDE to run the simulations of retrieval of NO_2 with TROPOMI instrument. My primary objective was to assess the impact of some instrumental errors, in particular instrument noise, stray light and spectral mis-registration, on the retrieved NO_2 total column. On this task I was working together with Marco Esposito from Cosine and with support of Johan de Vries from Dutch Space. With the progress of our research, more and more imperfections of the program were found. Even some errors were detected due to unreasonable results, and consequently also corrected. The final results of the analyses are therefore not totally applicable, but TIDE showed very good potential to be used in future work. The decision was reached to upgrade it with last missing details and afterwards repeat the analyses of the effect of instrumental errors. In April 2011, when I finished my stage at ESTEC, TIDE was still in incomplete phase; therefore, I did not have the opportunity to redo my work. TIDE is expected to be ready for further runs in autumn 2011.

The observations of NO_2 have been simulated above the Netherlands, which was covered with the matrix of 79 x 71 pixels. The second out of four spectral channels has been used, the one that covers the part of UV and visible light (310 – 496 nm). Preliminary results obtained from the study hereby presented show that the spectral mis-registration can contribute considerably to the NO_2 retrieval error. 10 pm mis-registration let the retrieval algorithm exceed the accuracy requirement of almost five

times. Noise causes an error of $11 - 12$ % which is also just above the requirement. Therefore, high signal to noise ratio is very important. Uniform stray light error is largely eliminated by the calibration. Wrong calibration causes the error of about 1% or less. The effect of uniform stray light has the smallest contribution to the error budget.

Although the results are not completely reliable and fully applicable for further analyses my work has proven to be important in the frame of development of the instrument. In addition to new knowledge and experiences I gained, I also helped to detect the error in the software and the 'bad' results encouraged the software developers to add missing algorithms.

After the upgrading of TIDE there are a lot of things to be done and tested with it. The effects of instrumental errors have to be assessed again but on a higher level. Test on isolated effects from clouds, tests for other channels (SWIR) and other trace gases (CO, CH_4, SO_2), and tests with non-uniform stray light are to be done.

Imaging spectroscopy or hyper spectral remote sensing is used in wide variety of applications, not only in atmospheric observations. With this technique detailed data on the materials and classes present on the surface of the Earth or other planets. It can also help us to discover the secrets of the Universe, remote galaxies, solar systems and their stars.

9   SLOVENSKI POVZETEK

V zadnjem obdobju so vse pogostejše in vse hujše vremenske ujme – suše, poplave, orkani, temperaturni ekstremi. Le-te naj bi bile posledica globalnega segrevanja ozračja, h kateremu veliko prispeva tudi človek s svojim delovanjem in načinom življenja. Antropogene klimatske spremembe že ogrožajo številne ekosisteme na Zemlji, zato so Združeni Narodi v devetdesetih letih prejšnjega stoletja sprejeli številne mednarodne konvencije, protokole in amandmaje o zmanjševanju izpustov toplogrednih plinov ter snovi, ki uničujejo ozonsko plast v atmosferi. Najpomembnejši so Dunajska konvencija o varstvu ozonskega plašča (1992), Montrealski protokol o substancah, ki škodljivo delujejo na ozonski plašč (1992) ter Okvirna konvencija Združenih narodov o podnebnih spremembah (1995) s Kjotskim protokolom o zmanjšanju izpusta ogljikovega dioksida in ostalih toplogrednih plinov (2002) (MOP, 2011). K vsem omenjenim sporazumom je pristopila tudi Slovenija.

Da bi lahko odgovorili na številna vprašanja, ki se ob tem problemu postavljajo, je ključnega pomena dobro poznavanje plinov, prisotnih v ozračju, kako se s časom spreminja njihova koncentracija ter kašne so kemijske reakcije med njimi. Za ocenjevanje in predvidevanje razvoja podnebnih sprememb je najpomembnejše redno globalno opazovanje sestave Zemljine atmosfere. To omogoča nadziranje izvajanja s konvencijami določenih pravil ter iskanje izvorov različnih emisij, boljše poznavanje kemijskih procesov v ozračju pa je zelo pomembno tudi za ugotavljanje vplivov, ki jih imajo ti na vreme in podnebje. Najbolj učinkovito sredstvo za pridobivanje potrebnih podatkov so satelitska opazovanja. Prednost satelitskih opazovanj pred opazovanji z Zemlje, letal ali raket je predvsem v bistveno večji količini podatkov, ki jih pridobimo v enakem časovnem intervalu ter v tem, da s sateliti pokrijemo tudi težko dostopna območja, kot so oceani, puščave, gorovja ter severni in južni pol. Sateliti lahko v enem dnevu posnamejo celotno zemeljsko oblo in s tem omogočajo dnevno spremljanje sprememb v celotni atmosferi. Današnja tehnologija zagotavlja tudi že dovolj veliko prostorsko ločljivost, da lahko iz posnetkov lociramo izvore posameznih plinov ter s tem določimo glavne onesnaževalce.

Satelitska opazovanja Zemljine atmosfere neprekinjeno potekajo že vse od leta 1960, ko je ameriška vlada izstrelila prvi meteorološki satelit TIROS 1 (Television and Infrared Observation Satellite), katerega glavna naloga je bilo snemanje porazdelitve oblakov. Od takrat do danes so vesoljske agencije po svetu izstrelile vrsto satelitov, namenjenih opazovanju različnih lastnosti ozračja.

V diplomski nalogi so predstavljene osnove slikovne absorpcijske spektroskopije sodobnih satelitskih instrumentov namenjenih zaznavanju koncentracije posameznih plinov v atmosferi, tudi tistih, ki se pojavljajo le v sledovih, a igrajo pomembno vlogo pri kakovosti zraka ali prispevajo k učinku tople grede. Še delujoča instrumenta, ki delujeta po principu absorpcijske spektroskopije, sta SCIAMACHY (SCanning Imaging Absorption spectroMetre for Atmospheric CartograpHY, ESA, 2002) in OMI

(Ozone Monitoring Instrument, NASA, 2004). ESA pa v sodelovanju z nizozemskimi nacionalnimi vesoljskimi in meteorološkimi instituti že razvija nov instrument TROPOMI (Tropospheric Ozone-Monitoring Instrument), katerega izstrelitev je predvidena za leto 2014. Nizozemska je sodelovala tudi pri razvoju prvih dveh omenjenih instrumentov.

Med petmesečno prakso, ki sem jo opravljala v Evropskem vesoljskem centru za raziskave in tehnologijo (European Space Research and Technology Centre – ESTEC) Evropske vesoljske agencije (ESA) na Nizozemskem, sem sodelovala v projektu razvoja instrumenta TROPOMI. Moja naloga je bila z računalniškim programom, ki simulira delovanje instrumenta, oceniti vpliv instrumentalnih pogreškov na natančnost zajema vertikalnih profilov atmosferskih plinov. V nadaljevanju so povzete teoretične osnove ter predstavljeni rezultati opravljenih analiz.

9.1   Spektroskopija

Spektroskopija ali spektralna analiza je veda, ki preučuje elektromagnetni spekter – različne valovne dolžine elektromagnetnega valovanja. Spektroskopija se uporablja zlasti v kemiji, fiziki in astronomiji. Z njeno pomočjo lahko določimo kemijsko sestavo teles, ki elektromagnetno valovanje oddajajo (emisijske črte), prisotnost in koncentracijo posameznih kemijskih elementov in spojin v mediju, skozi katerega svetloba potuje (absorpcijske črte) ter strukturo molekul in atomov. V astronomiji s spektroskopijo določajo lastnosti nebesnih teles, kot so npr. oddaljenost, zgradba, hitrost in smer premikanja ter (ne)prisotnost atmosfere.
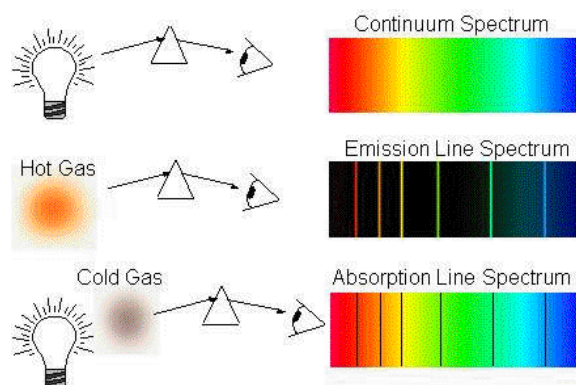
Slika 1: Neprekinjen spekter bele svetlobe (zgoraj), emisijske črte, s katerih prepoznamo lastnosti telesa, ki oddaja svetlobo (na sredini) ter absorpcijske črte (spodaj), preko katerih prepoznamo lastnosti medija, skozi katerega je svetloba potovala.

Za analizo kemijske sestave atmosfere se uporablja absorpcijska spektroskopija. Instrument, spektrometer, zazna Sončevo svetlobo, ki se je odbila od zemeljskega površja ter na svoji poti od Sonca do satelita dvakrat prečkala atmosfero. Hkrati satelit meri tudi valovanje, ki od Sonca do njega prihaja direktno. Na poti skozi plinasto atmosfero pride do interakcije svetlobe z delci in molekulami – svetloba se sipa in absorbira. Pri sipanju se svetloba, ki pade na delec, razprši na vse strani, pri

absorpciji pa se določene valovne dolžine vpijejo in ne nadaljujejo poti. Spekter, ki ga spektrometer zazna, ni zvezen, ampak je prekinjen s črnimi črtami, ki predstavljajo absorbirane valovne dolžine. Vsak plin v atmosferi absorbira točno določene valovne dolžine, pravimo, da ima svoj spektralni podpis. S primerjavo spektra, ki ga dobimo z opazovanjem elektromagnetnega valovanja proti Zemlji ter direktno proti Soncu, lahko na podlagi absorpcijskih črt določimo vrsto ter koncentracijo posameznih plinov v atmosferi. Z ustreznim preračunom dobimo tudi vertikalne profile plinov.
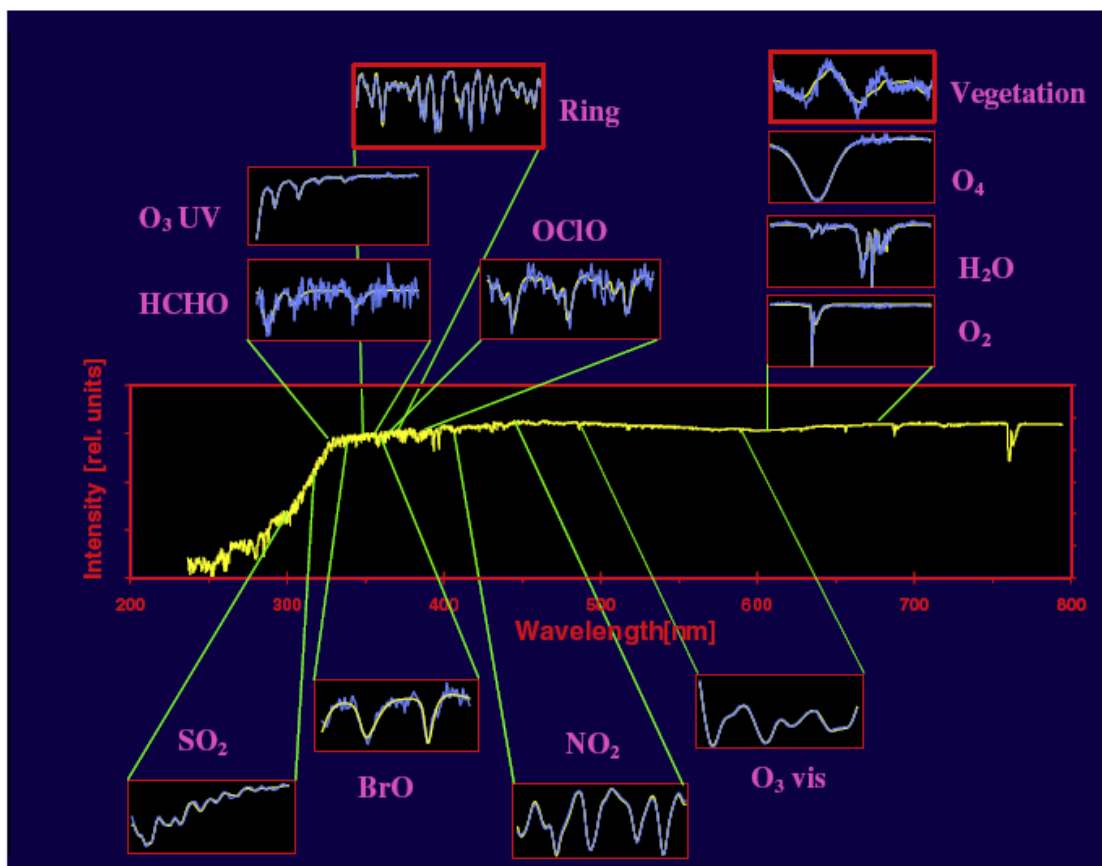
Slika 2: Izbor območij valovnih dolžin za spektralno analizo različnih atmosferskih plinov. V okencih rumene linije označujejo absorpcijski spekter posameznih plinov, svetlo modra črta pa predstavlja absorpcijo, zaznano s spektrom, opazovanim z instrumentom GOME.

9.2   Viri pogreškov pri meritvah s spektrometrom

Tako kot vse tehnike daljinskega zaznavanja so tudi spektrometrične meritve plinov v atmosferi podvržene raznim pogreškom, ki jih lahko razdelimo v tri skupine:

- pogreški direktnega modela,
- pogreški inverznega modela in
- instrumentalni pogreški.

Pogreški direktnega modela so tisti pogreški, ki se pojavijo pri izračunu sevalnosti (radiance) in obsevanosti (irradiance). Pri sipanju in absorpciji v atmosferi kot tudi pri vplivu oblakov, aerosolov in površin na elektromagnetno valovanje gre za zapletene procese, ki jih niti najboljši modeli ne morejo aproksimirati brez napak. Praviloma pa ti pogreški pri izračunu profila plina znašajo manj kot 1 % RMS. V primeru, da računamo dolgoročen trend iz opazovanj z istim instrumentom, lahko te pogreške zanemarimo, kar pa ne velja, kadar primerjamo dva različna sistema.

Pogreški inverznega modela so posledica dejstva, da za preračun sevalnosti v geofizikalne parametre potrebujemo a-priori oceno vertikalne porazdelitve preučevanega plina v atmosferi, ker tako lahko upoštevamo popravke zaradi temperature in tlaka. Po velikosti so pogreški inverznega modela relativno majhni, saj praviloma znašajo manj kot 1 % RMS.

Znatnejši vpliv na natančnost opazovanj pa imajo instrumentalni pogreški. Najpomembnejši med njimi so razpršena svetloba (stray light), šum (noise) in netočna registracija valovnih dolžin (mis-registration). Vpliv vseh je bil ocenjen s simulacijami instrumenta TROPOMI. Rezultati in analize so v celoti predstavljeni v nalogi v poglavju 7, povzeti pa v nadaljevanju.

Razpršena svetloba je neželeno sipano valovanje znotraj instrumenta; ločimo spektralno in prostorsko razpršeno svetlobo. Spektralna je tista razpršena svetloba, ki pade na slikovne elemente, namenjene beleženju valovanja drugih valovnih dolžin, in je po navadi posledica odsevov znotraj instrumenta, prostorska razpršena svetloba pa je tista svetloba, ki doseže teleskop, a je njen vir zunaj trenutnega vidnega polja. Šum je prav tako neželen signal, ki kvari kvaliteto podobe na detektorju. Šum je slučajni pogrešek in ga ne moremo povsem odstraniti. Ločimo tri vrste šuma: termični ali temni tok elektronov (dark current), šum fotonov (shot noise) ter bralni šum (readout noise). Šum fotonov je posledica neenakomernega padanja fotonov na površino senzorja. Bralni šum nastaja pri merjenju naboja slikovnega elementa. Termični tok nastane zaradi toplote in je odvisen od delovne temperature senzorja. Spektralna netočna registracija je napaka v ločevanju valovnih dolžin – vpadni signal zabeležimo z napačno valovno dolžino. Ta pogrešek lahko eliminiramo s spektralno kalibracijo.

9.3   Diferencialna optična absorpcijska spektroskopija (DOAS)

Diferencialna optična absorpcijska spektroskopija je metoda, ki omogoča kontinuirane meritve povprečnih koncentracij vrste atmosferskih plinov vzdolž izbrane poti v atmosferi. Po principu metode DOAS delujejo vsi obravnavani satelitski instrumenti, to je TROPOMI, OMI, GOME in SCIAMACHY. Pri tej tehnologiji se v ozkih spektralnih pasovih opazuje elektromagnetno valovanje proti Zemlji ter direktno proti Soncu. Spekter, ki ga dobimo z opazovanjem direktno proti Soncu, imenujemo referenčni spekter, saj se sprejemnik nahaja na satelitu, torej nad atmosfero, in tako EM valovanje ni bilo podvrženo reakciji s plini. Obe opazovanji, referenčno in tisto proti Zemlji, se nato primerjata in na podlagi razlik lahko določimo gostoto posameznih plinov vzdolž poti, ki jo je svetloba

prepotovala od Sonca do Zemlje ter nazaj do sprejemnika. Do razlik med obema spektroma (proti Soncu in proti Zemlji) pride, ker plini v Zemljini atmosferi absorbirajo določene valovne dolžine. Osnovna enačba absorpcijske spektroskopije je Lambert-Beerov absorpcijski zakon, ki je opisan v poglavju 4.3.

Rezultat DOAS analize je gostota določenega plina sešteta vzdolž poševne poti, ki jo je EM valovanje opravilo skozi atmosfero. Če želimo pridobiti vertikalni profil gostote plina, moramo poznati številne parametre, kot so geometrija opazovanja, položaj satelita, položaj Sonca, opazovana valovna dolžina, in vertikalni profili plina, zračnega tlaka ter temperature.

9.4   Analize in rezultati

Vse analize so bile opravljene s programom TIDE, ki simulira delovanje hiperspektralnega spektrografa TROPOMI in ga je v okviru projekta razvoja tega instrumenta razvilo nizozemsko podjetje Dutch Space. Program deluje na principu omrežnega računalništva, saj je simulacija hiperspektralnega instrumenta računsko zelo zahtevna naloga. Združuje računske module različnih skupina znanstvenikov, ki sodelujejo v projektu, ter tako omogoča vpogled v končne rezultate vsem sodelujočim.

Opravljene so bile tri analize, in sicer vpliv šuma, vpliv razpršene svetlobe in vpliv netočne registracije valovnih dolžin na zajem gostote dušikovega dioksida. Opazovanja so bila simulirana nad območjem Nizozemske, ki ga je pokrila matrika z 79 x 71 slikovnimi elementi (piksli). Stanje atmosfere (temperatura, tlak, oblačnost, porazdelitev plinov ter aerosolov, …) je bilo enako, kot je bilo 5. januarja 2007 ob 13:00 – zmerno onesnaženo z delno raztrgano oblačnostjo (glej Figure 33). Uporabljen je bil drugi spektralni kanal od štirih, ki zajema del ultravijolične ter vidno svetlobo (310 – 496 nm). Program sam kot rezultat ni podal iskanih vplivov pogreškov, pač pa gostoto izbranega plina, sešteto vzdolž poševne poti EM valovanja, kot bi jo izmeril instrument z danimi nastavitvami v danih atmosferskih pogojih. Vplive pogreškov sem izolirala tako, da sem med seboj odštela rezultate različnih simulacij. Primerjava z gostoto plina, ki je bila uporabljena kot vhodni podatek, zaradi nedokončanosti programa ni bila smiselna. Simulacija je bila obremenjena s številnimi pogreški zaradi nepopolnih algoritmov, zato sem s pogreški obremenjene rezultate primerjala s t.i. referenčnimi rezultati, ki sem jih dobila s simulacijo zajema s popolnim instrumentom, brez instrumentalnih pogreškov. Za vsak pogrešek sem izračunala kvadratni koren vsote kvadratov (RMS) relativnih odstopanj na vseh slikovnih elementih matrike.

Pri analizi vpliva razpršene svetlobe je bil analiziran vliv enotne razpršene svetlobe, ki je odvisna le od zaznanega signala ne pa tudi od valovne dolžine in kota gledanja, saj program še ni dodelan do te stopnje. Izvedla sem simulacije z različnimi stopnjami razpršene svetlobe v inverznem modelu, med

tem ko je le-ta v direktnem modelu ostala ves čas enaka pričakovani vrednosti 1,8 %. Rezultati so predstavljeni v preglednici 1:

Preglednica 1: Vpliv različnih stopenj razpršene svetlobe na stolpec NO₂.

Delež razpršene svetlobe [%]	0,9	1,8	3,6	7,2
Vpliv na NO₂ [%]	0,1	0,0	0,6	1,6

V primeru, ko je bila v obeh modelih uporabljena enaka stopnja razpršene svetlobe, se je njen vliv v celoti eliminiral. Zelo majhen je bil vpliv tudi pri dvakrat večji oziroma dvakrat manjši stopnji, kjer je znašal manj kot 1 %. Če bi pri izračunu gostote NO₂ stopnjo razpršene svetlobe ocenimo za štirikrat večjo kot je v resnici, znaša vliv te napake 1,6 %.

V primerjavi z vplivom razpršene svetlobe je vliv šuma na opazovanja precej večji – znaša dobrih 11 % za lastnosti instrumenta, kakršne bodo ob izstrelitvi satelita (BOL – beginning of life), ter dobrih 12 %, če upoštevamo spremembe v instrumentu, do katerih naj bi prišlo tekom let obratovanja (EOL – end of life). Stanje instrumenta ob koncu obratovalne dobe je ocenjeno na podlagi izkušenj s predhodnimi instrumenti (OMI, GOME) in se od izhodiščnega dizajna razlikuje v sedemkrat večjem termičnem toku in v za 10 % zmanjšani optični prepustnosti.

Predpostavila sem, da tudi stopnja oblačnosti vpliva na analizirana pogreška, saj se spremenita albedo ter sipanje svetlobe. Vrednosti sem razdelila glede na štiri stopnje oblačnosti – brez oblakov, z malo oblaki, oblačno ter z gostimi oblaki. Izkazalo se je, da oblačnost ne vpliva bistveno na vpliv šuma, po pričakovanju pa je nanjo občutljivejši vpliv razpršene svetlobe. Le-ta je največji na območjih z gosto oblačnostjo, najmanjši pa tam, kjer je oblakov malo. Rezultati so zbrani v preglednici 2.

Preglednica 2: Vpliv šuma in razpršene svetlobe na zajem NO₂ v odvisnosti od gostote oblakov.

	Brez oblakov	Malo oblakov (0 - 0.33)	Oblačno (0.33 - 0.66)	Gosti oblaki (> 0.66)	Celotno območje
Šum BOL [%]	11.91	10.18	11.88	11.84	11.11
Šum EOL [%]	13.02	11.03	12.91	12.79	12.08
SL[*] 0.9% [%]	0.09	0.08	0.10	0.23	0.10
SL 3.6% [%]	0.62	0.48	0.68	1.69	0.64
SL 7.2% [%]	1.57	1.19	1.67	4.13	1.61
Šum (BOL) + SL 3.6% [%]	12.64	10.50	12.40	12.87	11.63

[*] SL = razpršena svetloba (ang. stray light)

Z namenom ocenitve vpliva netočne registracije valovnih dolžin je bilo narejenih pet testnih primerov z različno velikimi napakami pri zaznavanju prave valovne dolžine – 10 pm, 50 pm, 100 pm, 300 pm in 500 pm. Ugotovljeno je bilo, da je vpliv netočne registracije valovnih dolžin zelo velik že, če valovno dolžino ocenimo za 10 pm narobe, saj le-ta znaša približno 50 %. Kot lahko vidimo iz grafa na sliki Figure 41 (stran 64), je pogrešek večji za območja z nižjo koncentracijo NO_2.

Če povzamem rezultate, iz opravljenih analiz vidimo, da je potrebna zelo visoka točnost pri registraciji različnih valovnih dolžin, vpliv šuma v spektrometru znaša okrog 10 %, vpliv razpršene svetlobe pa je približno za faktor 10 manjši, okrog 1 %.

Eden izmed pogojev, ki naj bi mu TROPOMI zadostil, je, da skupen vpliv instrumentalnih pogreškov na opazovanja gostote atmosferskih plinov naj ne bi znašal več kot 10 %. Iz rezultatov bi lahko sklepali, da trenutna zasnova instrumenta ne omogoča zadostitve tega pogoja, vendar vemo, da je program za simulacijo delovanja instrumenta še vedno v fazi razvoja, celo med izvajanjem analiz so bile odkrite nekatere napake in pomanjkljivosti, zato je krivda za 'slabe' rezultate najverjetneje na strani programa. Rezultati so spodbudili razvijalce programa, da ga dodelajo in dodajo manjkajoče algoritme. Trenutno poteka nadgradnja TIDE, ko bo zaključena, se bodo analize ponovile.

10   BIBLIOGRAPHY

Andrews, David, G. 2010. An Introduction to Atmospheric Phisiscs, second edition. Cambridge University Press.

Ashdown, I. 2002. Photometry and Radiometry – A tour guide for computer graphics enthusiasts. Heart Consultants Limited.
http://www.helios32.com/Measuring%20Light.pdf (14.1.2011).

Atmosphere Observation.
http://science.jrank.org/pages/596/Atmosphere-Observation.html (8.12.2010).

Atmospheric Sciences, University of Illinois at Urbana-Champaign – Satellite and Radar Remote Sensing.
http://www.atmos.illinois.edu/research/06remotesens.html (21.6.2011).

Aura atmospheric chemistry. NASA.
http://aura.gsfc.nasa.gov/index.html (17.3.2011).

Bhartia, P.K.2002. OMI Algorithm Theoretical Basis Document, Volume II. OMI Ozone Products. NASA Goddard Space Flight Center Greenbelt. Maryland, USA.
http://www.knmi.nl/omi/documents/data/OMI_ATBD_Volume_2_V2.pdf (5.9.2011).

Brohede, S. 2002. Differential Optical Absorption Spectroscopy – How does it work and what can it measure.
http://home.elka.pw.edu.pl/~rgraczyk/DOAS.pdf (9.12.2010).

Buscaglione, F. 2011. GMES Sentinel-5 Precursor System Requirement Document (SRD). For Official Use. ESA.

Cartage. Radiation Laws.
http://www.cartage.org.lb/en/themes/sciences/astronomy/Modenastronomy/Interactionoflight/RadiationLaws/RadiationLaws.htm (26.6.2011).

de Vries, J. 2010. TIDE and Scene Generator Description. Leiden. Dutch Space.

de Vries, J., Laan, E.C., Escudero-Sanz, I., Visser, H., Absen, I., Jongma, R.T., Levelt, P.F., Veefkind, J.P., Dobber, M. 2007a. From OMI and SCIAMACHY to TROPOMI: recent improvements in sun backscatter atmospheric composition measurements. 2007 joint EUMETSAT meteorological satellite conference and the 15th American meteorological society (AMS) satellite meteorology & oceanography conference, 24-28 September 2007, Amsterdam, The Netherlands.
http://www.knmi.nl/omi/documents/publications/proceedings/2007EUMETSAT_Paper_FromOMItoT ROPOMI.pdf (18.3.2011).

de Vries, J., Laan, E.C., Hoogeveen, R.W.M., Jongma, R.T., Absen, I., et al. 2007b. TROPOMI: Solar backscatter satellite instrument for air quality and climate. Proceedings SPIE Europe Remote Sensing, Florence (Italy), 17 - 20 September 2007.
http://www.knmi.nl/omi/documents/publications/proceedings/SPIE_2007_6744A-8_TROPOMI_Firenze_final_20aug2007.pdf (5.7.2011).

ESA Earthnet online.
http://earth.esa.int/ers/ (7.9.2011).

Fischer, J., Baumback, M., Grossmann, J., and Antoniades, J. 1998. Comparison of low-cost hyperspectral sensors. Imaging spectrometry IV. San Diego: p. 23-30.
http://www.brandywineoptics.com/pubs/SPIE1998.pdf (26.6.2011).

GRSS - Geoscience and Remote Sensing Society. 2009. Lidar for Atmospheric Trace Gas Detection.
http://www.grss-ieee.org/technical-resources-2/lidar-for-atmospheric-trace-gas-detection/ (3.9.2011).

Gottwald, M., Bovensmann, H., Lichtenberg, G. et al. 2006. SCIAMACHY, Monitoring the Changing Earth's Atmosphere. Freiburg: DLR, Institut für Methodik der Fernerkundung (IMF).

GSU – Giorgia State University. Hyperphysics.
http://hyperphysics.phy-astr.gsu.edu/hbase/atmos/blusky.html (26.6.2011).

Hefei Institute of Physical Science, Chinese Academy of Sciences.
http://english.hf.cas.cn/r/ResearchPrograms/AtmosphericOptics/ (26.7.2011).

Javed, M. U. 2009. Total DOAS Measurements in Bremen. Bremen, Universität Bremen.

Jørgensen, R. N. 2002. The VTTVIS Line Imaging Spectrometer - Principles, Error Sources, and Calibration. Roskilde, Riso National Laboratory.

Kelder, H. 2008. SCIAMACHY, GOME and OMI. Presentation given at University of Technology Eindhoven, The Netherlands.
http://earth.esa.int/atmostraining2008/Tue_kelder_scia-omivs1.pdf (9.12.2010).

KIT. Tracing Greenhouse Gases.
http://www.kit.edu/visit/pi_2011_5303.php (29.6.2011).

KNMI - The Royal Dutch Meteorology Institute. The GOME ozone monitoring instrument.
http://www.knmi.nl/gome_fd/doc/gomeintro.html (30.8.2011).

Liou, K. N. 2002. An introduction to Atmospheric Radiation. Second Edition. USA, Academic Press, An imprint of Elsevier Science: p. 1-36, 65-114.

Lyndon State College, Survey of Metrology Class Notes.
http://apollo.lsc.vsc.edu/classes/met130/notes/chapter1/vert_temp_all.html (19.12.2010).

MOP - Ministrstvo za okolje in prostor. Konvencije. (Ministry of the Environment and Spatial Planning. Conventions.)
http://www.konvencije.mop.gov.si/ (14.9.2011).

Mullard Space Science Laboratory. Detector Physics Group. Noise sources in a CCD.
http://www.mssl.ucl.ac.uk/www_detector/optheory/darkcurrent.html (5.9.2011).

NASA. Aura – Understanding and Protecting the Air We Breathe.
http://www.nasa.gov/mission_pages/aura/spacecraft/omi.html (17.3.2011).

NFSI – Near and Far Sciences for Illinois. Spectroscopy.
http://nfsi-server.yerkes.uchicago.edu/FTProot/spectroscope/Spectroscopy/basics1.htm#bright%20line (29.11.2010).

OMI – Ozone Monitoring Instrument.
http://www.knmi.nl/omi/research/instrument/optic.php?tag=full (5.9.2011).

Oštir, K. 2006. Daljinsko zaznavanje. Ljubljana, Inštitut za antropološke in prostorske študije ZRC SAZU (Remote Sensing. Ljubljana, Institute of Anthropological and Spatial Studies, Scientific Research Centre of the Slovenian Academy of Sciences and Art).

Palazzi, E. 2008. Retrieval of trace gases vertical profile in the lower atmosphere combining Differential Optical Absorption Spectroscopy with radiative transfer models. Dottotato di ricerca, Università degli Studi di Bologna.

PCO. Noise – general.
http://www.pco.de/fileadmin/user_upload/db/download/pco_cooKe_kb_noise_general_0504.pdf (14.12.2010).

Physics 2000, A University of Colorado at Boulder Website.
http://www.colorado.edu/physics/2000/cover.html (17.3.2010).

Richter, A. 2006. Differential optical absorption spectroscopy as a tool to measure pollution from space. Spectroscopy Europe: p. 14 – 21.
http://www.doas-bremen.de/paper/spec_euro_06_richter.pdf (9.12.2010).

SKP – Slovenski kemijski portal.
http://www.kemija.org/index.php/domov/25-okoljecat/68-pomen-atmosfere (17.11.2010).

Smith, G. 2009. Gene Smith's Astronomy Tutorial – Stellar Spectra. University of California, San Diego. Center for Astrophysics and Space Sciences.
http://casswww.ucsd.edu/public/tutorial/Stars.html (14.12.2010).

Stein Zweers, D.C., Veefkind, J.P., Sanders, A.J., Sneep, M., de Haan, J.2011. Latest aerosol algorithm developments for OMI and TROPOMI. KNMI.
http://presentations.copernicus.org/EGU2011-12143_presentation.pdf (2.9.2011).

The Science of Doom. The Sun and Max Planck Agree. 2010.
http://scienceofdoom.com/2010/06/01/the-sun-and-max-planck-agree/ (26.6.2011).

TROPOMI.
http://www.tropomi.eu/TROPOMI/Instrument.html (30.7.2011).

Urbas, A., Esposito, M., and de Vries, J. 2011. Effects of Instrumental Errors in the Retrieval of Anthropogenic Gas Distribution from Satellite. EARSeL 7th SIG-Imaging Spectroscopy Workshop. Edinburgh.

Veefkind et al. 2011. TROPOMI on the ESA Sentinel-5 Precursor: Global Observations of the Atmospheric Composition for Climate and Air Quality Applications. Geophysical Research Abstracts, Vol. 13, EGU2011-11629-1. EGU General Assembly 2011.
http://meetingorganizer.copernicus.org/EGU2011/EGU2011-11629-1.pdf (30.7.2011).

Virginia Tech. The Chemistry Hypermedia Project – On-line resources for students, educators, and scientists. Optical Spectrometers.
http://www.files.chem.vt.edu/chem-ed/optics/selector/spectrom.html (27.6.2011).

Wagner, T., Beirle, S., Deutschmann, T., Eigemeier, E., Frankenberg, C., Grzegorski, M., Liu, C., Marbach, T., Platt, U., Penning de Vries, M. 2008. Monitoring of atmospheric trace gases, clouds, aerosols and surface properties from UV/vis/NIR satellite instruments. Journal of Optics A: Pure and Applied Optics.
doi:10.1088/1464-4258/10/10/104019